

PRECISION CUTTING IN CNC TURNING MACHINES

by

BÜLENT DELÝBAĐ

Submitted to the Graduate School of Engineering and Natural Sciences

in partial fulfillment of

the requirements for the degree of

Master of Science

SABANCI UNIVERSITY

Spring 2002

© Bülent Deliba° 2002

All Rights Reserved

PRECISION CUTTING IN CNC TURNING MACHINES

APPROVED BY:

Assistant Prof. Dr. ERHAN BUDAK
(Dissertation Supervisor)

.....
Assistant Prof. Dr. AHMET ONAT

.....
Assistant Prof. Dr. AYHAN BOZKURT

DATE OF APPROVAL:

ACKNOWLEDGMENTS

I would like to express my deepest appreciation to my advisors, Assistant Prof. Dr. Erhan Budak and Assistant Prof. Dr. Gokhan Goktug, for the guidance, encouragement, and feedback they provided to me during the thesis process.

I especially would like to thank my mother, brother and sisters for their support and encouragement. Also I would like to add the special thanks to Ernur Karadogan, Ahmet Gurbuz, Yasser El-Kahlout, Ozkan Ozturk, Evren Kivanc and agdas Arslan for their help for me in the progression of the thesis. Lastly, I would like to thank my friends in my faculty for their encouragement.

LIST OF TABLES

2.1	Classification of geometric errors and causes.....	11
3.1	Roundness measurement of master gauge.....	30
3.2	Diameter measurements of master gauge.....	31
3.3	Linear measurements of master gauge in CNC machine.....	32
3.4	Results of rotational measurements of master gauge in CNC machine	35
3.5	Comparision of diameter measurements of workpiece betwee compensated and uncompensated case.....	37
3.6	Rotational measurements of master gauge in CNC machine.....	39
5.1	Calculation of PID parameters by using Ziegler-Nichols first method.....	55
5.2	PID parameters of PBCD control.....	55
5.3	Feedback normalization of PBCD.....	57
5.4	Example1: Comparision of measurements between PBCD control cutting and no control cutting.....	59
5.5	Example2: Comparision of measurements between PBCD control cutting and no control cutting.....	61
5.6	Example3: Comparision of measurements between PBCD control cutting and no control cutting.....	63
5.7	Example4: Comparision of diameter measurements between PBCD control cutting and no control cutting.....	65
5.8	Example 5: Dynamic position control results of PBCD.....	69

1.1	2
1.2	2
1.3	3
1.4	4
1.5	5
2.1	9
2.	11
2.	11
2.	12
2.	12
2.4	12
2.5	13
2.6	14
2.7	16
2.	17
2.	17
2.	18
2.	18
2.	19
2.	19
2.11	20
3.1	22
3.2	22
3.3	Tilting (Wobbling) error..... 24
3.4	Deformation error..... 26
3.5	Moment diagram at cutting..... 26
3.6	Weight of workpiece..... 27
3.7	Straightness error of CNC machine..... 29
3.8	Roundness error of master gauge along the length..... 30
3.9	Diameter variation of master gauge along the length..... 31
3.10	In process measurements in CNC lathe..... 32
3.11	Linear measurements..... 32

3.12	Laser measurements with respect to chuck end position.....	34
3.13a	Maximum positive tilting error.....	35
3.13b	Maximum negative tilting error.....	35
3.14	Linear measurements of gauge with respect to measurement location.....	35
3.15	Comparison between compensated and uncompensated case.....	37
3.16a	Uncompensated cutting.....	38
3.16b	Compensated cutting.....	38
3.17	Rotational measurements.....	38
3.18	Rotational measurement results of gauge.....	39
3.19	Effect of side straightness on measurement.....	40
4.1	Hysteresis loop of piezo stack actuator.....	43
4.2	Creep of open loop piezo stack actuator.....	44
4.3	Wheatstone bridge circuit.....	48
4.4	Amplifier circuit for piezo feedback.....	48
4.5	Piezo housing.....	49
4.6	Real displacement versus amplifier voltage graph.....	50
4.7	Principle of piezo housing.....	51
4.8	EMCO 155 PC Turn machine	53
5.1	PID control	54
5.2a	Ziegler-Nichols first method.....	55
5.2b	Ziegler-Nichols second method.....	55
5.3	Feedback normalization of PBCD.....	57
5.4	Constant position control of PBCD.....	58
5.5	(Example1) Comparison of roundness error between PBCD control and no control.....	60
5.6	(Example2) Comparison of roundness error between PBCD control and no control.....	62
5.7	(Example3) Comparison of roundness error between PBCD control and no control.....	64
5.8	Diameter variation of workpiece between no control and constant position control case.....	66
5.9	Dynamic position control of PBCD.....	67
5.10	Dynamic position control results of PBCD.....	69

Abstract

Precision cutting, considering the time, cost and flexibility of the production, has been one of the major goals in manufacturing. Especially using new technological tools such as linear motors, laser and piezoelectric actuators in cutting operations to increase the accuracy of the workpieces produced, is becoming more popular day by day.

In this thesis, a new precision cutting system is developed to decrease the basic workpiece errors (straightness, roundness, diameter error, etc.) for commercial CNC lathes in a cheaper way. In order to characterise the CNC lathe, a laser displacement sensor is used. A mechanical design with piezo stack actuator and tool tip, i.e. piezo based cutting device (PBCD), is inserted on the turret of CNC lathe to give both static and dynamic finish cutting operation of PBCD. FEA (Finite Element Analysis) tool is used at the design stage of PBCD. The controller of PBCD is PID (Proportional Integrate Derivative) control that is running in the dSPACE software. In dynamic operation of PBCD, instantaneous angular position of CNC lathe spindle is specified by means of the rotary encoder. And it is used in the control loop for active elimination of roundness errors of cylindrical workpieces during cutting operation. The results after assessment of the measurements of cylindrical workpieces are encouraging. In static operation of PBCD, the finish cutting decreases the roundness error at an amount of at least 30% with respect to the operation without control of PBCD.

In most CNC turning machines, if cutting conditions such as cutting speed and feed, tool geometry and vibration are not changed, the workpiece geometric errors are mostly repeatable. So it may not be needed to measure the geometric errors of the same workpiece produced at the same cutting conditions after each cutting operation. Especially in mass production, all cutting conditions and workpiece produced are same. So, the PBCD would be very useful tool in mass production regarding the repeatability of workpiece geometric errors.

retim sistemlerindeki temel hedeflerden birini oluřturmaktadır. zellikle retilen iřparalarnn dođruluđunu artrmak iin yaplan kesme iřlemleri srasnda kullanlan lineer motor, lazer ve piezoelektrik a

Bu tezde, piyasadaki CNC torna tezgahlar üzerinde retilen iřparalarnn hatalarnn

kesme sistemi geliřtirilmiřtir. CNC torna tezgahnn karakterizasyonu iin lazer uzaklk lm sensr kullanld. Piezostak akřuatr, kesme kalem ucu ve mekanik tasarmdan oluřan piezo temelli kesme aleti (PBCD) son kesme pasosunu hem statik hemde dinamik almak iin, CNC torna tezgah taret üzerine monte edilmiřtir. PBCD nin tasarm ařamasnda sonlu elemanlar analizi (FEA) kullanlmřtır. PBCD nin kontrolr dSPACE yazlmnda kořulan PID (Proportional Integrate Derivative)

torna eksen motorunun enkoderi silindirik iřparalarnn yuvarlaklk hatalarnn aktif eliminasyonu iin kontrol dngs iine alnmřtır. Silindirik iřparalarnn makine dř muřtur. PBCD ile yaplan statik son kesme pasosu yuvarlaklk hatasndaki azalmann en az 30 % oldugunu gstermektedir.

Bir ok CNC torna makinalarnda, kesme hz ve pasosu, kalem geometrisi ve titreřimi

Dolaysyla ayn paralarn ayn durumlarda kesimi ile oluřan para geometrik hatalarn, her kesim iřleminden sonra lmeye gerek kalmayabilir. zellikle seri retimde, btn kesme r. Dolaysyla, PBCD seri retim iin ok yararlı bir ara olabilir.

TABLE OF CONTENTS

ACKNOWLEDGEMENTS.....	Iv
LIST OF FIGURES.....	V
LIST OF TABLES.....	Vi
ABSTRACT.....	Viii
OZET.....	Ix
TABLE OF CONTENTS.....	X
1 INTRODUCTION.....	1
2 SURFACE ERRORS.....	9
2.1 Surface irregularities.....	9
2.2 Modelling of roundness.....	10
2.2.1 Eccentricity.....	11
2.2.2 Ellipticity (Ovality).....	11
2.2.3 Trilobe error.....	16
2.2.4 Wavieness.....	17
2.2.5 Combination of errors.....	18
2.3 Combination of roundness harmonics.....	19
3 CHARACTERISATION OF CNC THE TURNING MACHINE.....	21
3.1 Sources of errors in CNC turning machines.....	22
3.1.1 Set-up errors.....	22
3.1.2 Position error.....	25
3.1.3 Thermal error.....	25
3.1.4 Deformation error.....	26
3.1.5 Deformation error under weight.....	27
3.1.6 Wearing error.....	27
3.1.7 Control error.....	28
3.1.8 Vibration error.....	28
3.1.9 Measurement error.....	28
3.2 Characterisation of workpiece machined in CNC machine.....	28
3.3 Cylindrical master gauge.....	29
3.3.1 Characterisation of cylindrical master gauge.....	29
3.3.2 Measurement of cylindrical master gauge in CNC machine.....	31

3.3.2.1	Linear measurements.....	32
3.3.2.2	Rotational measurements.....	38
4	DEVELOPMENT OF THE SYSTEM (PBCD).....	42
4.1	Piezo stack actuator.....	42
4.1.1	Hysteresis.....	42
4.1.2	Creep.....	43
4.1.3	Stroke.....	44
4.1.4	Stiffness.....	44
4.1.5	Resonant frequency.....	45
4.1.6	Electrical capacitance.....	45
4.1.7	Power consumption.....	45
4.2	Piezo voltage amplifier.....	45
4.2.1	Specification of piezo voltage amplifier.....	45
4.2.2	Limitation of piezo voltage amplifier.....	46
4.3	Piezo sensor amplifier circuit.....	48
4.4	Tool tip.....	48
4.5	Mechanical housing.....	49
4.6	dSPACE 1102 hardware and software.....	52
4.7	P.C.....	52
4.8	CNC Turning machine.....	52
5	EXPERIMENTS AND RESULTS.....	54
5.1	Control of piezo stack actuator.....	54
5.2	Constant position control of PBCD.....	56
5.3	Dynamic position control of PBCD.....	66
6	CONCLUSION AND FUTURE WORK.....	70
	REFERENCE LIST.....	73
	APPENDIX.....	77

CHAPTER 1

INTRODUCTION

Nowadays requirements for accuracy and precision demand high quality in manufacturing. But, the manufacture of components is not always possible to be produced at ideal geometric shape and accuracy. Hence, tolerances for deviations from nominal sizes are to be defined. Demands on higher reliability and quality force the designer to manufacture parts inside these tolerances. So producers must respect these tolerances when producing a new product.

Due to the increasing demand of precision parts and devices in many industries such as optics, computers, automotive and aerospace etc, it may, in general, be possible to achieve the required precision operations at high accuracy by using expensive manufacturing equipments. In addition to these costly equipments, using a secondary finishing operation such as grinding or polishing may significantly reduce the productivity and introduce set-up errors. There are some ultra precise turning machines, which can produce parts at micro level accuracy. Special machine tool manufacturers produce these machines. But they are very costly compared to standard machine tools used in the industry. These turning machines have to be operated in a temperature controlled, vibration free and stable environment.

Turning is one of the most commonly used processes where metal is removed by rotating the workpiece with respect to a tool. The workpiece is held in a chuck that is clamped to the spindle. The tool is held in a tool post that is mounted on a cross-slide, which provides radial tool movement. If the workpiece is long, both of the ends are held by the chuck and tailstock. The cross-slide is held on the top of a carriage that has motion along the axis between spindle and tailstock centres. Conventional lathes have single motor that rotates the spindle via gearbox and belts (Figure 1.1).

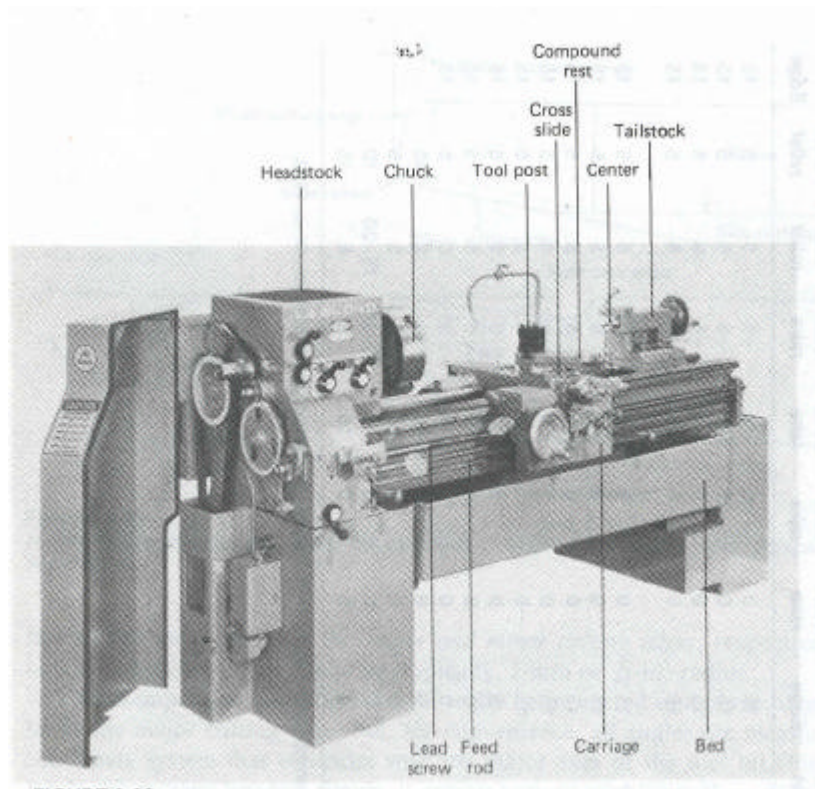


Figure 1.1 Conventional lathe

In CNC (Computer Numerical Control) turning machines, unlike conventional ones, the feed and spindle speeds are programmed within computer programs (Figure 1.2). In these machines, the turret holds the tools. The turret may contain multiple (6-12) cutting tools.

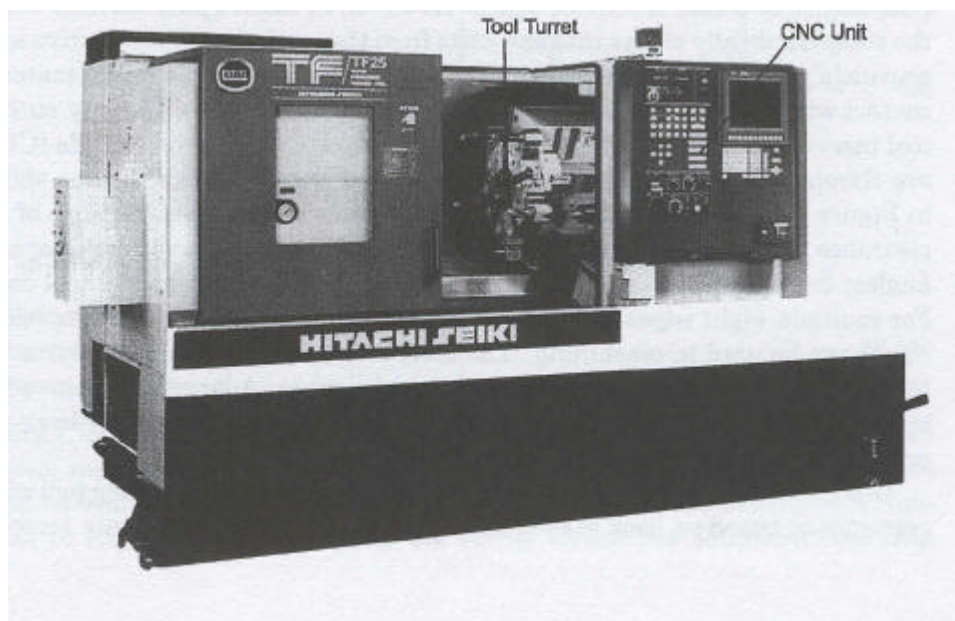


Figure 1.2 CNC Turning machine

The important parameters of turning machines are; spindle speed, feed rate, depth of cut and tool geometry (rake face, clearance face). Spindle speed is the angular speed of the rotating workpiece. Feed rate is the distance moved by the tool in an axial direction for each revolution of the workpiece. Depth of cut is the thickness of metal removed from the workpiece measured in a radial direction.

Rake face is the surface of the tool on which the chip flows.

Clearance face is the surface that is behind of the rake face of the tool (Figure 1.3).

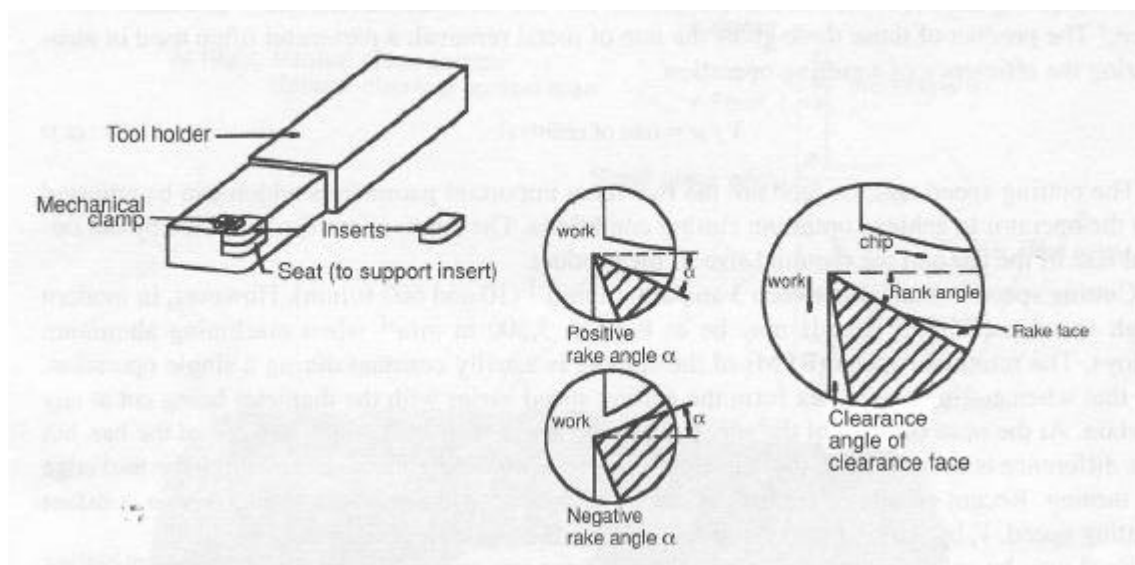


Figure 1.3 Cutting tool geometry

In turning operation, the tool and workpiece are exposed to the cutting forces in three directions. These are feed force, tangential force and radial force (Figure 1.4) [28], [29], [30], [17].

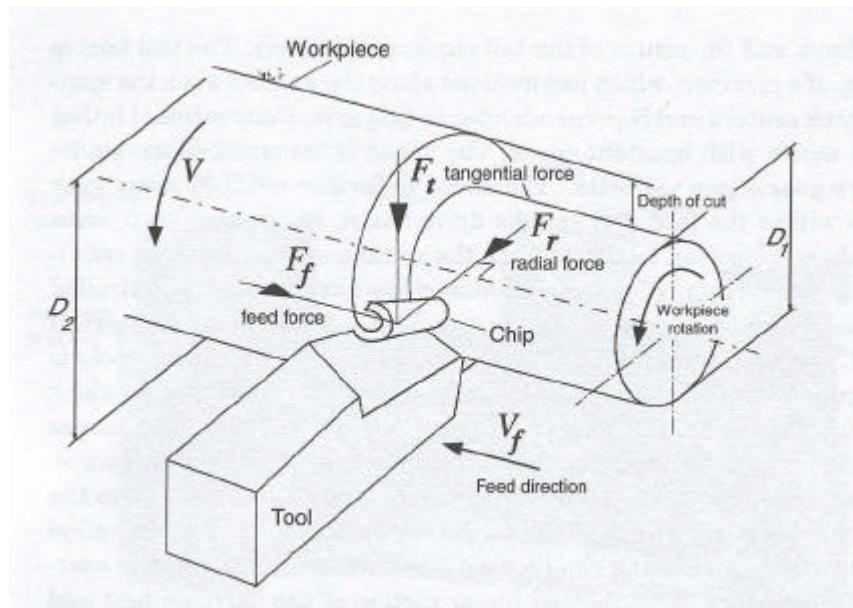


Figure 1.4 Cutting forces

Precision turning, considering multiple manufacturing processes (lapping, polishing after turning), may be more effectively performed by a special operation called single point diamond turning (SPDT). SPDT is a process that uses a monocrystalline diamond as the cutting tool. It is a well-established fabrication process for shaping high quality optical surfaces on metals, polymers and crystals. It has the capability of precision machining. The rigidity of the machine tools in SPDT operation is very significant. External vibration can easily affect the quality of diamond turned workpieces. Therefore all motors and drive mechanisms must be dynamically balanced and isolated to eliminate vibration between tool and workpiece. Figure 1.5 shows typical CNC SPDT machines. [31], [32], [33], [34].



Figure 1.5 CNC Diamond turning machines

In industry, most of the CNC turning machines are not so precise and accurate. So that, these need to be modified if high precise and accurate products are desired. The modification of these machines would be cheaper than buying a new high precise machine. Therefore inserting independent systems on CNC turning machines are becoming much more efficient.

Various precision turning operations by using piezo stack actuators or servo systems have been investigated in the past. One of the earliest studies was implemented by Mergler and Sahajdak [1, 2]. They used a laser beam focusing on the workpiece to control the diameter of the cylindrical part. The displacement sensor that determines whether the focal point is on the right position of the workpiece surface or not, gives feedback to the servomechanism to control the slide, carrying both laser beam and cutting tool position to maintain the diameter of the part in feed direction. Since the displacement sensor depends on the carriage of the tool, the accuracy of the system is limited (Diameter variation 10 μm at a distance of 200mm along the feed) [3]. Wen-Hong Zhu et. al [4], [19] presented a piezo driven fast tool servo for precision turning of shafts on conventional CNC lathes. They designed a robust system to keep the tool tip at the desired location within the displacement sensor resolution (0.1 μm) and for compensating cutting force disturbances and hysteresis of the piezo actuator by using sliding mode controller. Their main aim was to increase the surface quality of the workpiece by finish cutting with the fast tool servo driven piezo stack actuator in diamond turning. They obtained a surface roughness value that can only be reached by grinding process. James Li et al. [5] developed an in-process measurement and control system in precision diamond turning in order to improve the roundness of the workpiece. For detecting roundness errors, three co-planar capacitance probes mounted on the machine were used. To give necessary control action, piezoelectric actuator was used by means of P-integrator controller. They demonstrated the reduction of the roundness error by more than one order of magnitude in aluminum machining with low depth of cut (1 μm). In [6] Jeong-Du Kim et al. showed a micro cutting device with piezo-electric actuator to control sub-micron depth of cut and compensate the waviness on the surface of the workpiece in face turning carried out on a precision lathe which was operated in a thermostatic and vibration free environment. Eddy current gap sensor and piezo-electric feedback were used to control the micro-depth control device with PI controller. The results showed

that the considerable amount of waviness error was eliminated on the surface profile of the workpiece. The implementation of an on-line measurement system for the evaluation of the cylindricity of the workpiece was presented by Shawky and Elbestawi [7]. They developed an on-line measurement system using three ultrasonic transducers, which have 5 μ m accuracy operating in wet environment cutting. Their goal was to reduce the quality control cost by the help of on-line assessment of workpiece geometry. In [9], ANN (Artificial Neural Network) is used to estimate the workpiece error depends on the geometric error, thermal induced error, cutting condition (feed, speed and depth of cut) and the motor currents. Based on the estimated error, the compensation is done by modifying the CNC codes. The model reduces the workpiece error down to $\pm 5 \mu\text{m}$ from $\pm 14 \mu\text{m}$. Also in this model only CNC code compensation was used since its cost would be lower than the other systems. Similarly, Chin-Hao Lo et al. [10] presented compensation scheme to correct repeatable thermally induced errors and geometric errors on a four-axis dual-spindle turning center by using optimum values of thermocouples and capacitance sensors. The real-time error compensation control reduces the machine error by 90 percent. Sang-soon Ku et al. [23] designed a three degree of freedom, piezo electric actuator based, nano-metric precision positioner, in order to eliminate the effect of friction and backlash of a machine tool during diamond turning of brittle materials such as glass, ceramic, zinc sulfide and germanium at low feed rates and depth of cut. The control of the positioners is a neural network with standard PID control algorithm. James F. Cuttino et al. [25] presented a device designed to extend the capacity of existing machines for the production of nonaxisymmetric workpieces with fast tool servo using single-point diamond turning machines. They used two controller schemes; an optimised PID control and a technique that utilize a dynamic compensator module which samples the hysteric voltage/displacement relationship in real time and modifies the effective gain accordingly in conjunction with the linear controller. Their empirical results showed 80 % reduction in the motion error caused by hysteresis.

Piezo electric actuators are also used in different cutting processes and measurement devices such as boring, taper turning and Coordinate Measuring Machine (CMM). Byung-Kwon Min et al. [20] developed a new type of boring tool (Smart Tool) to increase precision and flexibility at the boring station. Their main goal is to decrease the unwanted effects, which are mechanical vibration, poor part

quality and short tool life of boring process with high length to diameter ratio (L/D) of bars. They used an active tool-tip servo with piezoelectric actuator and position sensitive optical detectors for compensation of vibration and deflection occurred at boring process. They operated the system with position error less than 1µm for both step and sinusoidal position inputs. The implementation of piezoelectric actuator for on-line compensation of machining errors in precision boring of holes with high length to diameter ratio (L/D) is presented by D. Gao et al. [22]. Their design consists of a dual-concentric boring bar with one end outside piezoelectric actuator and inside strain gauge. The other end is a cutting insert. Because of the elastic deformation properties of long boring bar, they designed real time error compensation control by strain gauge deformation sensing feedback and piezoelectric actuator displacements accordingly. They obtained successful results (40 % roundness and diameter variation improvement). H. K. Fung et al. [8] showed an in-process error measurement, off-line error modelling, simulation and on-line stochastic error forecasting and compensation for roundness improvement in taper turning. They constructed the idea of evaluation of the roundness error as the difference between the ideal and actual depth of cut. The difference is measured by two optical encoders, one proximity sensor and a pre-calibrated master taper. The compensating action is given by piezoelectric tool post that consists of piezoelectric table and a tool holder. Their final achievement is between 24 % to 38 % roundness error improvements. R. Bansevicius et al. [24] proposed a piezo electric actuator based system for volumetric error compensation of multi degree of freedom systems (gripper of an industrial robot, probe of a CMM). They used piezoelectric actuators for two purposes in CMM. Piezoelectric actuator is used both in formation of signal in the contact with surface of the object to be measured and to correct the geometric error at probe of CMM.

The nanomachining instruments and micro-lathes are being developed by integrating these PZTs, sensors, mechanical and electrical components. Wei Gao et al. [26] constructed a nanomachining instrument. In this instrument, the workpiece is moved by PZT in two directions, while the tool is kept stationary during the cutting process. The workpiece is mounted at the end of PZT to generate the crossfeed and feed cutting motion. The capacitive sensor is mounted at the end of PZT in order to control the PZT motion. Two-force sensors were used at the back of the tool that is stationary to measure cutting and thrust forces during cutting. They tested the instrument in a temperature-controlled environment. Yuichi Okazaki et al. [27]

actuators, were nearly perfect linear sensitivity (pascal/mm) and less hysteresis loop.

In this thesis, a new micro cutting device (PBCD), which is mounted on the turret of CNC turning machine, is designed and tested. Main purpose of this research is to increase the precision of workpiece in conventional CNC turning machines by adding this micro cutting device that is operated independently from CNC machine drive.

CHAPTER 2

SURFACE ERRORS

2. 1. Surface Irregularities

Machining of products, regardless of the use of high precision tool, shows some irregularities on the surface. The irregularities are categorized, according to its wavy like properties (frequency, amplitude), into three main groups. These are surface roughness, waviness, and form error. The figure 2.1 shows the surface roughness, waviness and form error on the surface.

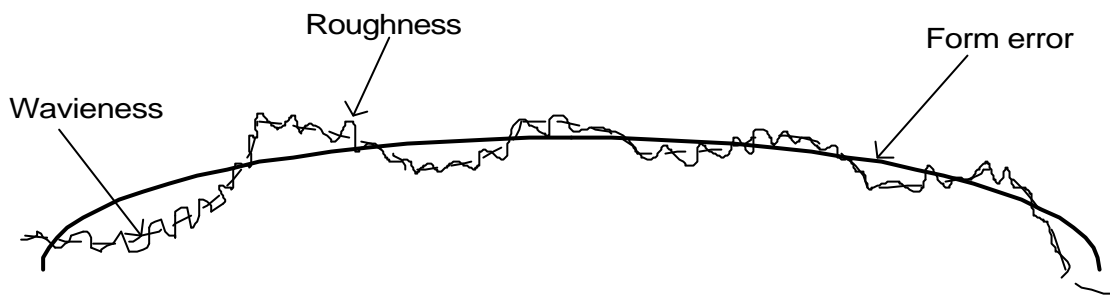


Figure 2.1 Geometric errors of surface

Surface roughness is the true air-metal boundary on the surface. It is generally defined, as the magnitude of wavelength per amplitude that is less than 10 of the surface waves. The surface roughness irregularities are mainly from the tool mark left on the machining such as turning, grinding and polishing. The only irregularity that does not change the general dimension of the product even if it is high is surface roughness.

Waviness errors are irregularities of longer wavelength on the surface. The magnitude of wavelength per amplitude is between 10 to 100 of the surface waves. An example of this error might be the effects caused by improper manufacturing such as vibration on the tool. Chatter marks on the surface are also kind of waviness.

If the surface irregularities wavelength per amplitude is in the order of 1000, then these errors are called form error. Causes of form irregularities stem from errors in guides and axes linearity, spindle error or thermal and mechanical distortion. Special name of form error in round workpieces at the cross-section is called roundness.

2. 2. Modelling of Roundness

Roundness is defined as the deviation of a workpiece from a perfect round part. A workpiece is described as round in a given cross section if all parts on the periphery are equidistant from a common center (Ecludian definition).

Geometric errors on a round workpieces are explained by using Fourier harmonic series. Actually by using FFT (Fast Fourier Transform), these geometric errors can be separated from each other.

$$r(\mathbf{q}) = R + \sum_{n=1}^{\infty} A_n \cdot \cos(n \cdot \mathbf{q} - \mathbf{j}_n) \quad 2-1a$$

or

$$r(\mathbf{q}) = R + \sum_{n=1}^{\infty} (a_n \cdot \cos(n \cdot \mathbf{q}) + b_n \cdot \sin(n \cdot \mathbf{q})) \quad 2-1b$$

Where R is the nominal radius,

$$A_n = \sqrt{(a_n^2 + b_n^2)}$$

A_n is the amplitude of the harmonic and,

$$\mathbf{j}_n = \tan^{-1}(b_n / a_n)$$

\mathbf{j}_n is the phase angle that is the orientation of the harmonic in the profile.

In Fourier expression, Fourier coefficient n is usually defined as the frequency coefficient that increases the frequency as n grows, but in roundness evaluation n refers to UPR (Undulation Per Revolution), which is the number of waves in one revolution. The only difference from frequency is the number of waves in one revolution not in one second. Actually we can relate both of them by using the angular speed (rpm) of the revolution.

By using the Fourier series expression it can be found how roundness errors occur on a workpiece and also it is possible to separate the geometric errors from each other with the help of UPR. Therefore the causes of each geometric error can be examined easily. Some geometric errors are given with corresponding causes below [\[17\]](#).

UPR	Effects	Causes
1	Eccentricity on a graph	Badly centered of w/p on spindle
2	Ovality(Ellipticity) of a workpiece	Tilting error of w/p on spindle
3	Trilobe effect on workpiece	Distortion from the jaws of chuck
4-5	Four and five lobed errors	Distortion from wrong clamping
5-20	Moderate lobed errors	Machine tool stiffness
20-50	Waviness	Marks due to vibration and chatter
50-1000	Higher lobed errors	Due to the high frequency vibration

Table 2.1 Classification of geometric errors and causes

2. 2. 1. Eccentricity

Eccentricity is defined as the misalignment between centre of rotation and the geometric centre of workpiece. (first harmonic of FFT). Eccentricity errors are usually due to the set-up errors not the real deviation. Eccentricity of a part is shown by its magnitude and angle from the center of rotation like vectorial quantity. Eccentricity is the first member of the Fourier series of the signal on the profile (Figure 2.2a, 2.2b).

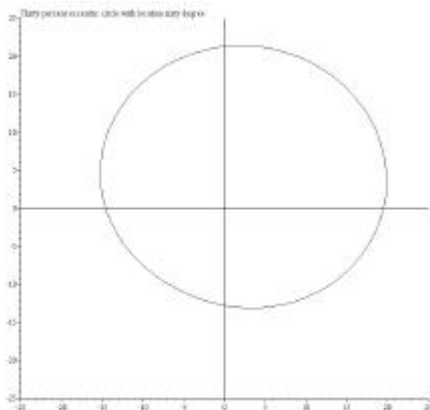


Figure 2.2a Eccentricity

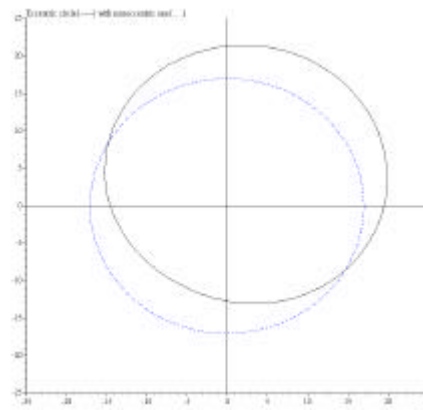


Figure 2.2b Eccentricity with true circle

2. 2. 2. Ellipticity (Ovality)

Ellipticity (Ovality) is the two lobed errors on a workpiece and it is the second harmonic of the Fourier series of the profile. It can be due to the tilting error of the spindle while rotating. Therefore, cylindrical parts are machined as an ellipse.

$$r_e(\mathbf{q}) = R + \sum_{n=1}^{\infty} A_n \cdot \sin(n \cdot \mathbf{q} + \mathbf{j}_n), \text{ if } R=20, A_n =2, n=2 \text{ and } \phi=0 \text{ then,}$$

$$r_e(\mathbf{q}) = 20 + 2 \cdot \sin(2 \cdot \mathbf{q} + \mathbf{j}),$$

Represents the polar graph with respect to the correct true circle of the figure 2.3a. And figure 2.3b shows the polar graph for different phase angles ($\delta=0, 90, 180, 270$). The different phase angles show that the irregularities may be on the some other locations of workpiece round cross-section.

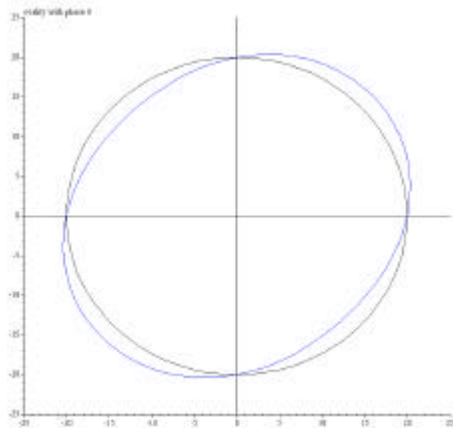


Figure 2.3a Ellipticity with true circle

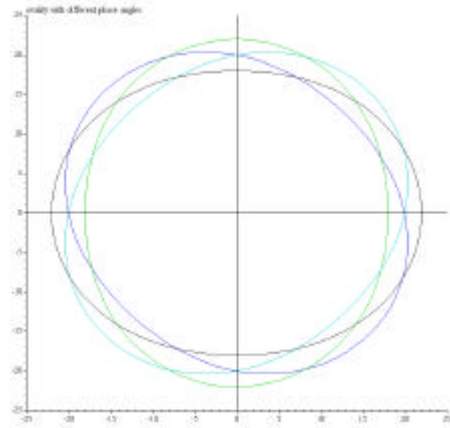


Figure 2.3b Ellipticity with different phases

Effect of centering on dimension in cutting:

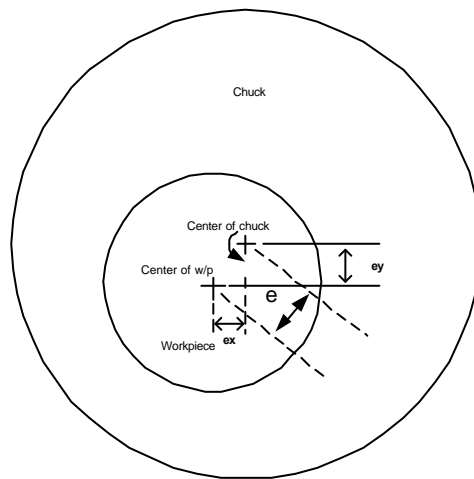


Figure 2.4 Effect of centering

If a cutting operation is done with a depth of cut (r) with centering;

$$e_y = e \cdot \cos(\mathbf{q} - \mathbf{q}_{\max}) \quad 2-2$$

$$r(\mathbf{q}) = R + e \cdot \cos(\mathbf{q} - \mathbf{q}_{\max}) \quad 2-3$$

Where R is nominal depth of cut and e is eccentricity error

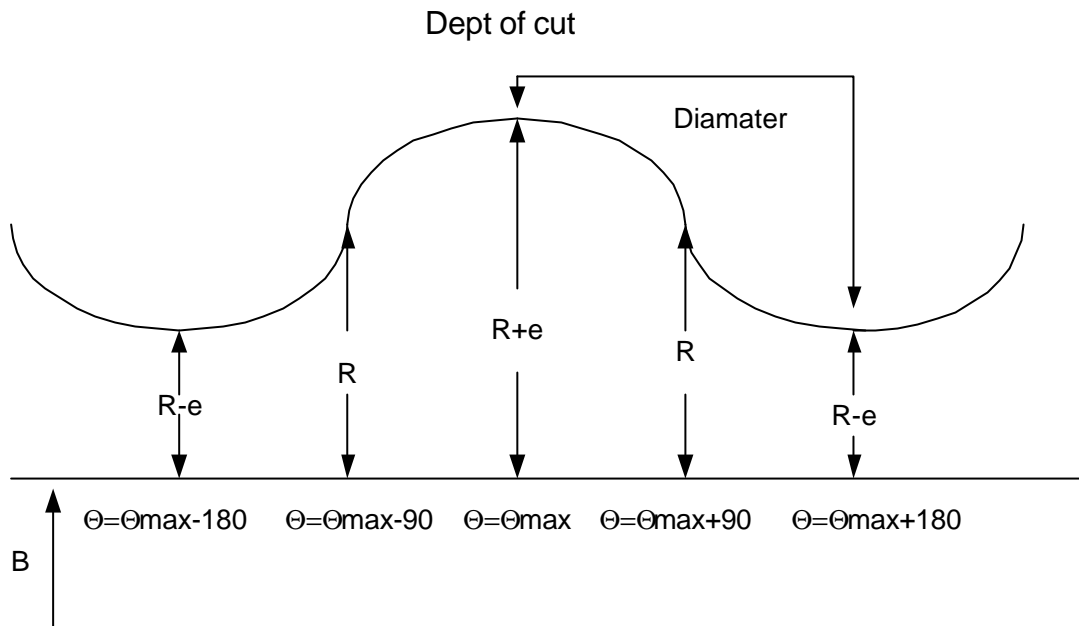


Figure 2.5 Depth of cut with centering

$$\text{Diameter1} = (R+e) + (R-e) + B = 2R + B$$

$$\text{Diameter2} = R + R + B = 2R + B$$

So diameter does not change from eccentricity value.

Also, how the roundness is affected from centering;

Since roundness is defined as the deviation of radius of the workpiece along the circumference (Figure 2.4, 2.5, 2.6).

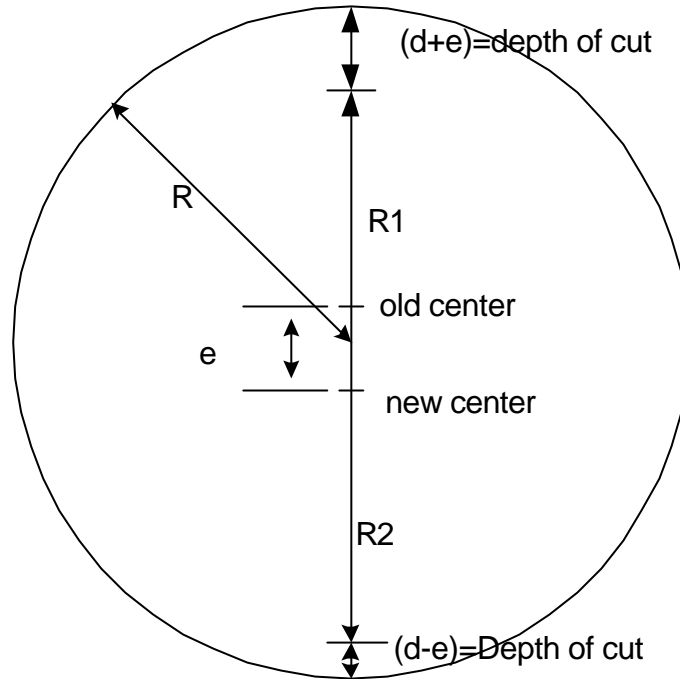


Figure 2.6 Effect centering on roundness

Where d is nominal depth of cut and e is eccentricity

Due to the old center;

$$\text{Radius1}=\text{R1}= R-(d+e) = R-d-e$$

$$\text{Radius2}=\text{R2}= R-(d-e) = R-d+e$$

Now according to new center;

$$\text{Radius1}=\text{R1}= R-d-e+e= R-d$$

$$\text{Radius2}=\text{R2}= R-d+e-e= R-d$$

So, centering does not affect the part dimension in cutting. The only change is the new center of the workpiece.

Effect of tilting on dimension in cutting:

Again the same analysis for tilting;

Depth of cut taken over part circumference;

$$r(\mathbf{q}) = R + l \cdot \mathbf{a} \cdot \cos(\mathbf{q} - \mathbf{q}_{t \max}) \quad 2-4$$

Where l is length of workpiece,

$\hat{e}_{t \max}$ is angle at which tilting is maximum at any section.

α is tilting (wobbling) angle

Again it is a constant plus sinusoidal variation (one wave along circumference).
Diameter and roundness value does not change when tilting exists.

Effect of both tilting and centering on dimension of workpiece

Since both centering and tilting have the same sinusoidal characteristics but different phase angles, the superposition of both errors would give the same characteristic of sinusoidal errors over the circumference.

Both centering and tilting have one UPR (Undulation Per Revolution) roundness. If they were added, the result would give one UPR roundness.

Since;

$$\text{Centering depth of cut} = d + e \cdot \cos(\mathbf{q} - \mathbf{q}_{c \max})$$

$$\text{Tilting depth of cut} = l \cdot \mathbf{a} \cdot \cos(\mathbf{q} - \mathbf{q}_{t \max} + \mathbf{j})$$

$$\text{Where } \mathbf{j} = \mathbf{q}_{t \max} - \mathbf{q}_{c \max} \text{ (phase angle between two waves)}$$

For example what is the diameter of workpiece after cutting:

$$\text{Diameter} = \left[R - (d + e \cdot \cos(\mathbf{q} - \mathbf{q}_{c \max})) + l \cdot \mathbf{a} \cdot \cos(\mathbf{q} - \mathbf{q}_{t \max} + \mathbf{j}) \right] + \left[R - (d + e \cdot \cos(\mathbf{q} - \mathbf{q}_{c \max} + \mathbf{p})) + l \cdot \mathbf{a} \cdot \cos(\mathbf{q} - \mathbf{q}_{t \max} + \mathbf{p} + \mathbf{j}) \right]$$

$$\text{Diameter} = \left[2 \cdot R - 2 \cdot d + e \cdot (\cos(\mathbf{q} - \mathbf{q}_{c \max}) + \cos(\mathbf{q} - \mathbf{q}_{c \max} + \mathbf{p})) \right] + \left[l \cdot \mathbf{a} \cdot (\cos(\mathbf{q} - \mathbf{q}_{t \max} + \mathbf{j}) + \cos(\mathbf{q} - \mathbf{q}_{t \max} + \mathbf{p} + \mathbf{j})) \right]$$

After eliminating the sinusoidal terms

$$\text{Diameter} = 2 \cdot D - 2 \cdot R$$

In conclusion, superposition of two same frequency sinusoidal waves gives the same frequency wave. So both centering and tilting does not change the dimension of workpiece in cutting operation. The only change is the center of the workpiece after cutting, and this result is no

$q_{c\max}$ (angle at which centering is max.), $q_{t\max}$ (angle at which tilting is max.).

2. 2. 3. Trilobe error

Trilobe roundness is a basic error that can be seen on the workpiece. It is basically three wavelengths on the workpiece in one revolution and it is the third component of the Fourier series expression of the profile. Most trilobe errors are because of the wrong clamping of the parts on the chuck of the tool in the lathe such as the excessive clamping load exerted by the jaws of the chuck on the workpiece. The jaws of the chuck applied on the workpiece are represented by a spring-damper system. Hence these points are more rigid than the other points that are free on the workpiece (Figure 2.7).

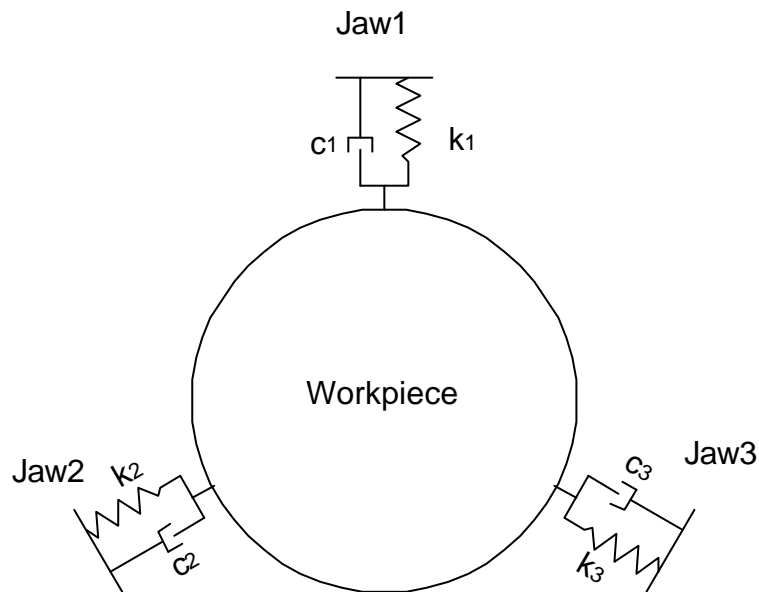


Figure 2.7 Trilobe effect at chuck

An example that explains trilobe error of a part is shown below. The polar graph of this shape has an equation

$$r_t(\mathbf{q}) = R + \sum_{n=1}^{\infty} A_n \cdot \sin(n \cdot \mathbf{q} + \mathbf{j}_n), \text{ if } R=20, A_n=2, n=3 \text{ and } \ddot{o}=0 \text{ then,}$$

$$r_t(\mathbf{q}) = 20 + 2 \cdot \sin(3 \cdot \mathbf{q} + \mathbf{j}),$$

Represents the polar graph with respect to the correct true circle of the figure 2.8a. And figure 2.8b shows the polar graph for different phase angles ($\delta=0, 90, 180, 270$).

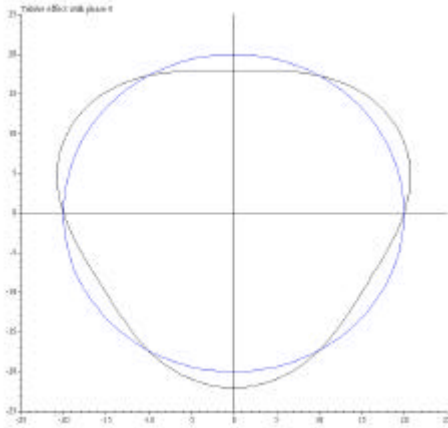


Figure 2.8a Trilobe with true circle

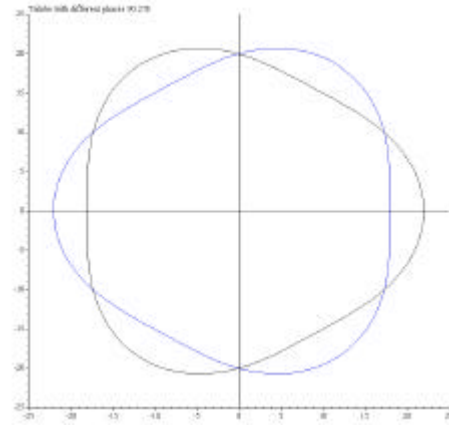


Figure 2.8b Trilobe with different phases

2. 2. 4. Waviness

Waviness errors are between the twentieth and fiftieth harmonics of the Fourier series equation on roundness profile. The main causes of these errors are chatter created at the cutting process. Chatter is a self-excited type of vibration that occurs in metal cutting operations. This associated vibration makes cutting forces periodically variable. When cutting forces reach considerable amplitudes, the machined surface becomes wavy. Chatter is easily recognised by the noise with this vibration and the marks left on the cutting surface. It an unacceptable situation in the cutting, hence it reduces the tool life and the surface quality of workpiece [35].

Here is an example that shows waviness error of a part. The polar graph of this shape has an equation

$$r_w(\mathbf{q}) = R + \sum_{n=1}^{\infty} A_n \cdot \sin(n \cdot \mathbf{q} + \mathbf{j}_n), \text{ if } R=20, A_n=2, n=50 \text{ and } \delta=60 \text{ then,}$$

$$r_e(\mathbf{q}) = 20 + 2 \cdot \sin(50 \cdot \mathbf{q} + \mathbf{j}),$$

Representing the polar graph with respect to the correct true circle of the figure 2.9a.

Also for different phase angles ($\delta=60, 180$), the polar graph becomes as in the figure 2.9b.

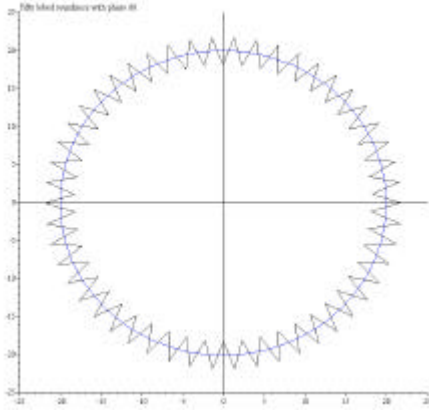


Figure 2.9a Waviness with true circle

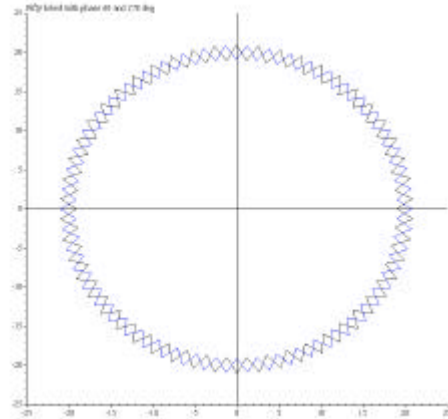


Figure 2.9b Waviness with different phases

2. 2. 5. Combination of errors (real case)

In a real round part all of these harmonics are combined on the workpiece profile. Below two Fourier harmonics are superposed with respect to correct circle is and corresponding FFT analysis is given in (Figure 2.10a, 2.10b). Two examples of this kind are demonstrated below; first one is the superposition of two harmonics (second and third).

The equation of first example:

$$r_c(\mathbf{q}) = 20 + 2 \cdot \sin(2 \cdot \mathbf{q} + \mathbf{j}_2) + 1 \cdot \sin(3 \cdot \mathbf{q} + \mathbf{j}_3),$$

$$\text{Where, } \mathbf{j}_2 = 0, \mathbf{j}_3 = 0$$

The other example is combination of five Fourier harmonics (second, third, fourth, fifth, and tenth) superposed on each other.

$$r_c(\mathbf{q}) = 20 + 1 \cdot \sin(2 \cdot \mathbf{q} + \mathbf{j}_2) + 0.8 \cdot \sin(3 \cdot \mathbf{q} + \mathbf{j}_3) + 1 \cdot \sin(4 \cdot \mathbf{q} + \mathbf{j}_4) + 0.7 \cdot \sin(5 \cdot \mathbf{q} + \mathbf{j}_5) + 0.4 \cdot \sin(10 \cdot \mathbf{q} + \mathbf{j}_{10}),$$

$$\text{where, } \mathbf{j}_2 = 0, \mathbf{j}_3 = 30, \mathbf{j}_4 = 150, \mathbf{j}_5 = 245, \mathbf{j}_{10} = 150$$

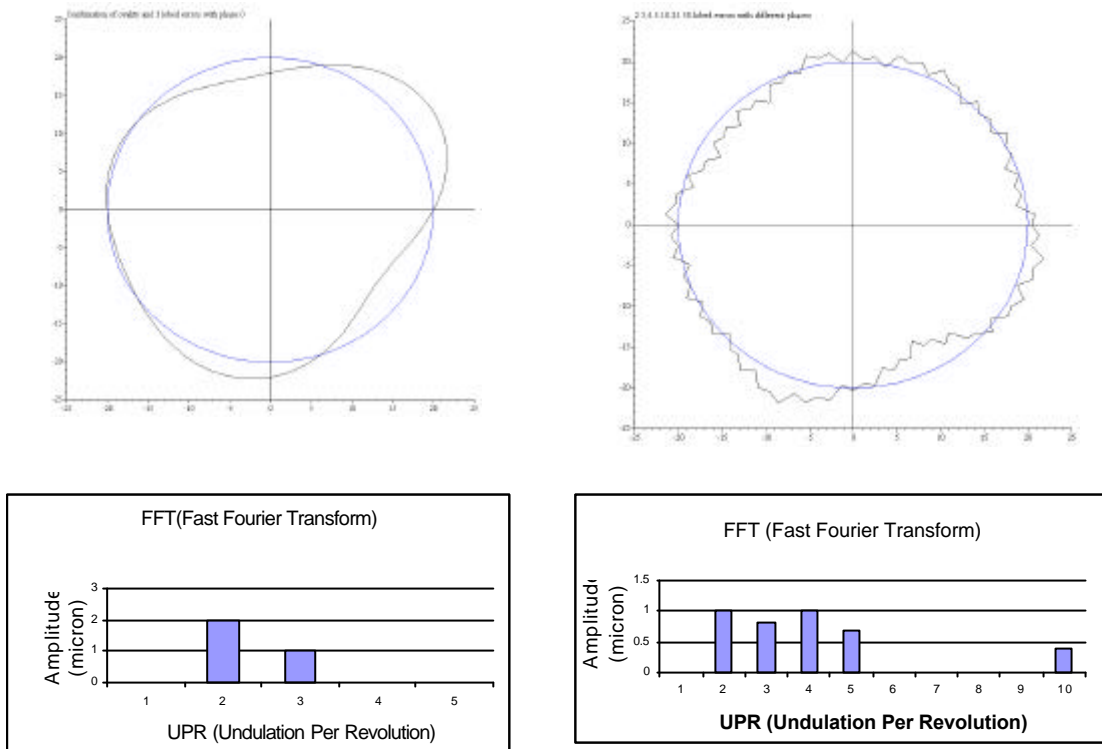


Figure 2.10a Combination of two harmonics with FFT analysis

Figure 2.10b Combination of five harmonics with FFT analysis

2. 3. Compensation of roundness harmonics

Since the roundness error of workpiece is categorized as its harmonics, applying the reverse of harmonics can compensate these errors. Of course this has to be in the micro level, since these errors are in the order of 1-2 micrometers. This compensation action must be applied dynamically, since CNC lathe chuck rotates (Figure 2.11). For example, if trilobe error is to be corrected at 1500 rpm angular speed, $(1500/60) = 25$ Hz (Spindle frequency), trilobe compensation frequency of $25 \cdot 3 = 75$ Hz actuation with specified amplitude must be supplied. Therefore an actuator, which can give that much of displacement with required bandwidth, is needed. Piezo stack actuator is selected to be the most suitable solution for this application. Besides these, the position of chuck must be known precisely to synchronize with the compensation action. Then the encoder of CNC spindle (chuck) motor must be used in a good synchronization with piezo stack actuator.

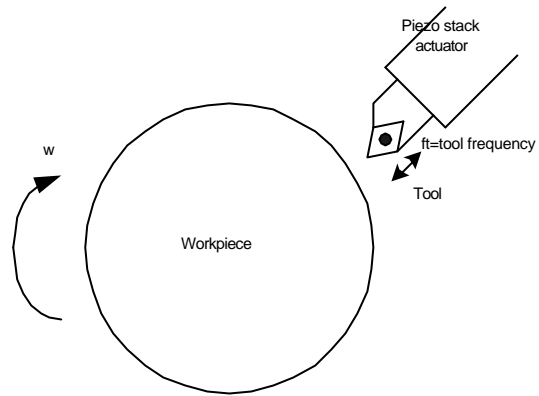


Figure 2.11 Compensation of harmonics by using piezo stack actuator

CHAPTER 3

CHARACTERISATION OF THE CNC TURNING MACHINE

In this chapter, characterisation of a CNC turning machine is investigated and necessary compensation and control action are carried out according to information obtained. Measurement, actuator, and computer methods used are clearly explained. The specifications of these elements are given.

Characterisation of CNC turning machine is very significant for the requirement of extracting the bulk errors such as axis linearity error, spindle motion error of the machine before implementing the precision cutting operations. Because some of these bulk errors are not compensated by suggested system (PBCD). So that characterisation of CNC turning machine is needed for separation of these errors.

In this chapter, the characterisation and possible sources of errors are examined by experimentally. The measurement and gauging system used in characterisation are explained. Also the possible surface error that is seen on workpiece is investigated.

3.1. SOURCES OF ERRORS IN CNC TURNING MACHINE

The accuracy and precision of CNC turning machines are affected due to variety of errors. All of these errors are combined (superposed) resulting in final irregularities on the surface of workpiece. Some of these errors occur during cutting operation caused by the process. On the other hand, some other errors are already there before cutting. Now, the sources of errors in CNC turning machine while in the cutting process are given:

$$e_{\text{total}} = e_{\text{set-up}} + e_{\text{position}} + e_{\text{cutting force}} + e_{\text{thermal}} + e_{\text{wear}} + e_{\text{weight of w/p}} + e_{\text{vibration}} + e_{\text{control}} + e_{\text{measurement}} \quad 3-1$$

The error components in equation (3-1) are explained in the following section;

3.1.1. Set-up errors ($e_{\text{set-up}}$)

These errors are basically due to spindle eccentricity and tilting that are explained below.

Chuck eccentricity

Eccentricity is defined as the misalignment between the center of rotation of spindle and the geometric center of the workpiece (Figure 3.1).

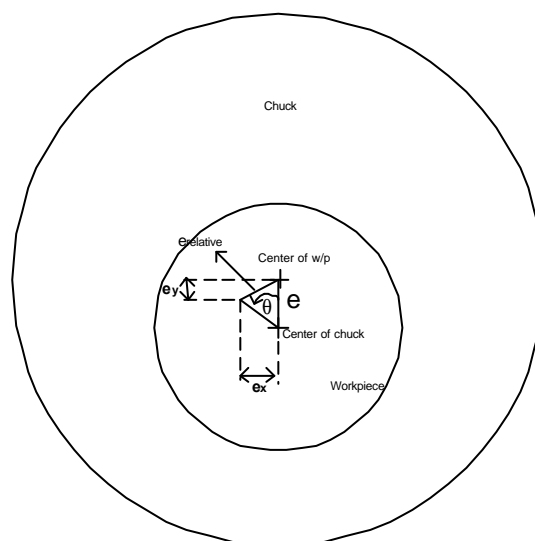


Figure 3.1 Chuck eccentricity

e is absolute error from center of chuck to the center of w/p.

$$e_y = e - e \cdot \cos \mathbf{q} \quad 3-2$$

$$e_x = e \cdot \sin \mathbf{q} \quad 3-3$$

$$e_{relative} = \sqrt{e_y^2 + e_x^2} \quad 3-4a$$

$$e_{relative} = e \cdot \sqrt{2 - 2 \cdot \cos \mathbf{q}} \quad 3-4b$$

$$e_{relativemax} = 2 \cdot e \text{ (for } \mathbf{q}=180^\circ) \quad 3-5$$

Which is the maximum displacement that is read from eccentricity error.

Note: This error does not change over the length of the workpiece. Because eccentricity is independent of axis of spindle.

The figure 3.2 shows the distance from a fixed point on the machine to the surface of the workpiece with only eccentricity of the workpiece. Laser displacement sensor assembled on the machine measuring distance to the workpiece while it is rotating is employed to depict the figure below.

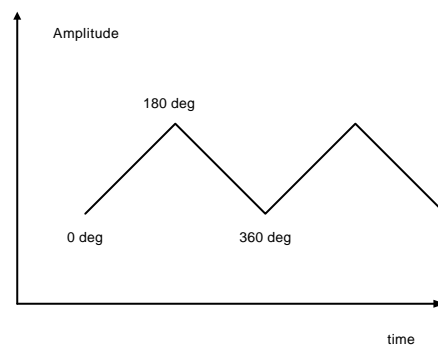


Figure 3.2 Effect of chuck eccentricity on measurement

Tilting (Wobbling) error of chuck workpiece assembly:

Tilting (Wobbling) error is the misalignment of the workpiece axis-of-rotation to the spindle axis of rotation (Figure 3.3).

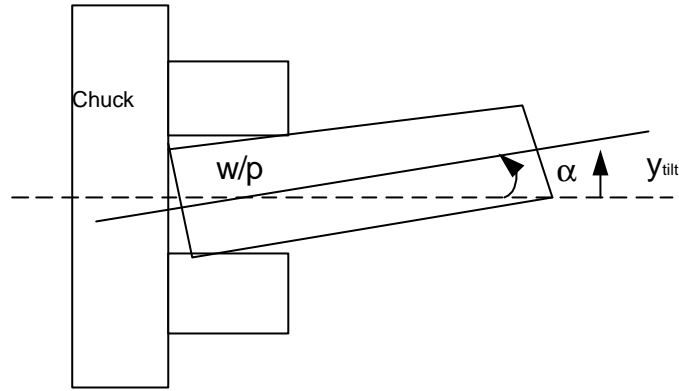


Figure 3.3 Tilting (Wobbling) error

$$y_{tilt} = L \cdot \sin \mathbf{a} \approx L \cdot \mathbf{a} \quad 3-6$$

$$\text{Maximum tilting error} = y_{tilt}(0^\circ) - y_{tilt}(180^\circ) = 2 \cdot L \cdot \mathbf{a}$$

The distance from fixed point on the machine to the surface of workpiece when only tilting of workpiece exists is same with eccentricity when chuck rotates.

Combination of eccentricity and wobbling error

Eccentricity and tilting errors are superimposed on the workpiece.

$$e_x = z \cdot \sin \mathbf{a} \cdot \sin \mathbf{q} \quad (\text{From Wobbling}) \quad 3-7$$

$$e_y = z \cdot \sin \mathbf{a} \cdot (1 - \cos \mathbf{q}) \quad (\text{From Wobbling}) \quad 3-8$$

Where z is the distance to the chuck along the workpiece.

$$e_{chuckx} = (e \cdot \sin \mathbf{q}) + z \cdot \mathbf{a} \cdot \sin \mathbf{q} \quad 3-9$$

$$e_{chucky} = e \cdot (1 - \cos \mathbf{q}) + z \cdot \mathbf{a} \cdot (1 - \cos \mathbf{q}) \quad 3-10$$

But they can not be added algebraically like above, because the location of eccentricity and tilting angles are different in both cases.

It will be shown later that, set-up errors do not create machining error if depth of cut is bigger than the eccentricity and wobbling error.

3. 1. 2. Position error (e_{position})

This is basically different from the offset errors of CNC machines. Throughout the thesis, position error is defined as the actual linearity of axes. (For machines under examined Z, X axes).

Linearity of the axis or column is defined as the straightness (deviation from true straight-line motion) of the static part. This depends on the overall geometry of the machine and applied loads.

Linearity is not a random error but a progressive error that means that it changes over the length of the machine element. Therefore, it is usually measured as micrometer deviation per mm length.

3. 1. 3. Thermal error (e_{thermal})

Thermal error is the form deviation of workpiece due to change of temperature and non-uniform temperature gradient of cutting processes. Temperature change induces thermal elastic strain, which is proportional to the product of the coefficient of expansion of the material and to the temperature change.

$$\mathbf{e}_t = \mathbf{a}_k \cdot \Delta T \quad 3-11$$

$$e_t = L \cdot \mathbf{e}_t \quad 3-12$$

Temperature deviation mainly affects the axes of machines. Using lubrication can minimize the temperature effects to the cutting tool and workpiece.

3. 1. 4. Deformation error ($e_{\text{cutting force}}$)

Deformation error is due to excessive cutting forces on the workpiece (Figure 3.4).

Analytical expression is explained like below:

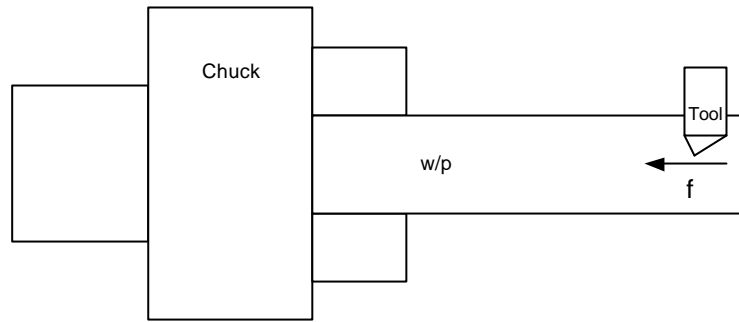


Figure 3.4 Deformation error

Moment diagram (Figure 3.5)



Figure 3.5 Moment diagram for cutting

Hence, the deformation equation

$$V_{\text{radialdeformation}} = \frac{(F_r \cdot x^3)}{(3 \cdot E \cdot I)} \quad 3-13$$

Where x is the distance to the chuck from cutting force location along the length of the workpiece.

$$\text{Radial cutting force} = F_r = K_r \cdot b \cdot t \quad 3-14$$

Where K_r is the force constant

b is the width of cut

t is the feed (mm/rev)

E is the Young modulus

I is the Moment of Inertia

$$I = \frac{P \cdot d^4}{64}$$

Note1: In this calculation chuck is considered to be rigid.

Note2: Direction of deformation is in radial direction.

3. 1. 5. Deformation error under weight (e_{weight})

Deformation error under weight is caused by the weight of the workpiece. The weight of the workpieces is represented by the distributed load shown below (Figure 3.6).

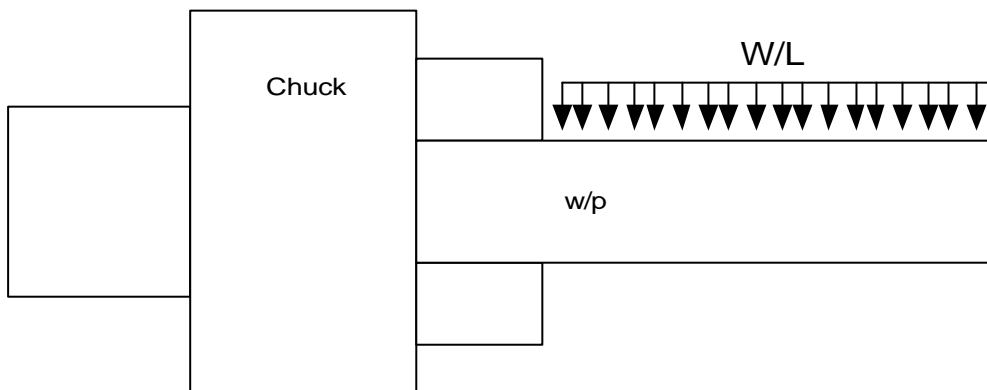


Figure 3.6 Weight of workpiece

Hence, the deformation equation becomes:

$$V_{\text{radialdeformation}} = \frac{(W \cdot x^3)}{(8 \cdot E \cdot I)} \quad 3-15$$

Where x is the distance to the chuck along the length of the workpiece.

3. 1. 6. Wear error (e_{wear})

Error due the wear of tool tip effects only surface roughness, so it creates negligible dimensional errors.

3. 1. 7. Control error (e_{control})

Control error mostly depends on the resolution of the control algorithm. Hence, if it is small enough, control error is negligible.

3. 1. 8. Vibration error ($e_{\text{vibration}}$)

Vibration error is due to the environmental condition of machining and cutting. Vibration gives a wavy surface on the workpiece.

3. 1. 9. Measurement error ($e_{\text{measurement}}$)

Measurement error is due to the uncertainty of the measurement. But it is generally negligible.

3. 2. Characterisation of workpieces machined in CNC machine

In order to find the general geometric errors, a cylindrical workpiece, which had nominal 38-mm diameter and 110 mm length, was machined in *EMCO PC TURN 155* CNC lathe with 0.1-mm depth of cut, 1500 rpm cutting speed with no tailstock support. Then, diameter of this workpiece was measured outside the CNC turning machine by *Aeroel* slit laser. The figure below shows the diameter variation of this part along its length with comparison to a cylindrical ground 150 mm length and 40 mm diameter round part. The red curve (machined in CNC) is changing approximately linearly (37.7824 mm to 37.8218mm) along its length from the chuck. The deviation is 40 micrometer, and this is maximum at the end of its length from chuck end position. On the other hand, blue curve has no linearly changing diametrical variation. This error is basically straightness error of the workpiece. This error is probably coming from the guide of CNC machine, but how it can be proved will be showed later by using laser measurement of perfect lapped gauge (Figure 3.7).

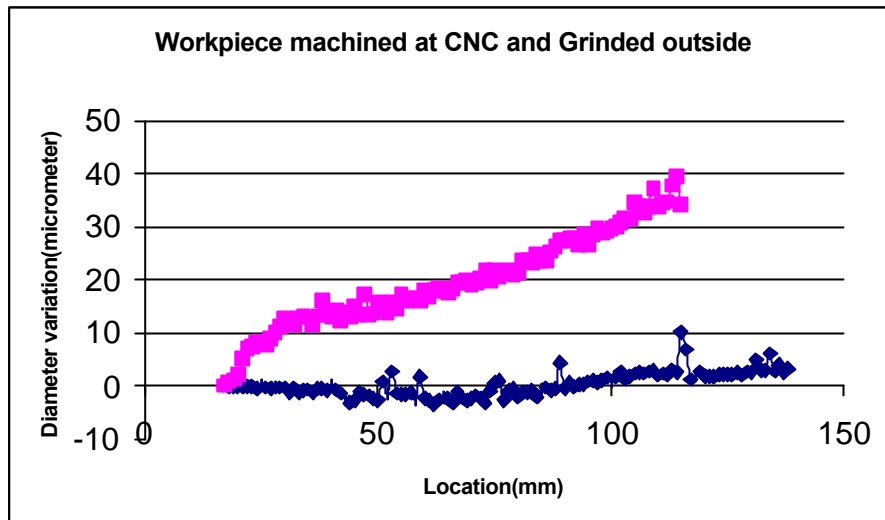


Figure 3.7 Straightness error of CNC machine

3. 3. Cylindrical master gauge (lapped)

3. 3.1. Characterisation of cylindrical master gauge (lapped)

In order to find bulk error of CNC lathe, a cylindrical master gauge was produced. The piece was lapped after turning. The master gauge has a good roundness value which is less than 0.3 micrometer, exact diameter value is 40.002 mm and diameter variation less than 2 micrometer over 80 mm gauge length. These values are measured and given by producer's company calibration laboratory with the help of their measurement instruments. This gauge is usually used as a master gauge for calibrations.

In order to find the whole characteristics of the master gauge, roundness measurement instrument (*Mitutoyo Roundtest, RA-116*) was used for measuring dimensional error of this gauge at different sections. Then, these errors are magnified to see the exact location of the errors. Hence, by using FFT (Fast Fourier Transform), separation of the errors was done with respect to their UPR (Undulation Per Revolution) values. Because of the inaccurate column of roundness measurement instrument, we can not measure cylindricity and linearity of this guide. But we can use *Aeroel slit laser* for measuring linearity by using diametric variation at different sections. These measurements are given below (Table 3.1, 3.2), (Figure 3.8, 3.9):

Roundness measurements of master gauge

Location of measurement from chuck (mm)	Roundness (Micrometer)	Maximum UPR Value	Amplitude of max. UPR (micrometer)
10	0.32	2	0.13
15	0.27	2	0.13
20	0.20	2	0.12
25	0.24	2	0.09
30	0.26	2	0.11
35	0.32	2	0.18
40	0.34	2	0.19
45	0.39	2	0.19
50	0.48	2	0.22
55	0.54	2	0.27
60	0.59	2	0.29
65	0.65	2	0.33
70	0.59	2	0.31
75	0.74	2	0.36

Table 3.1 Roundness measurements of master gauge

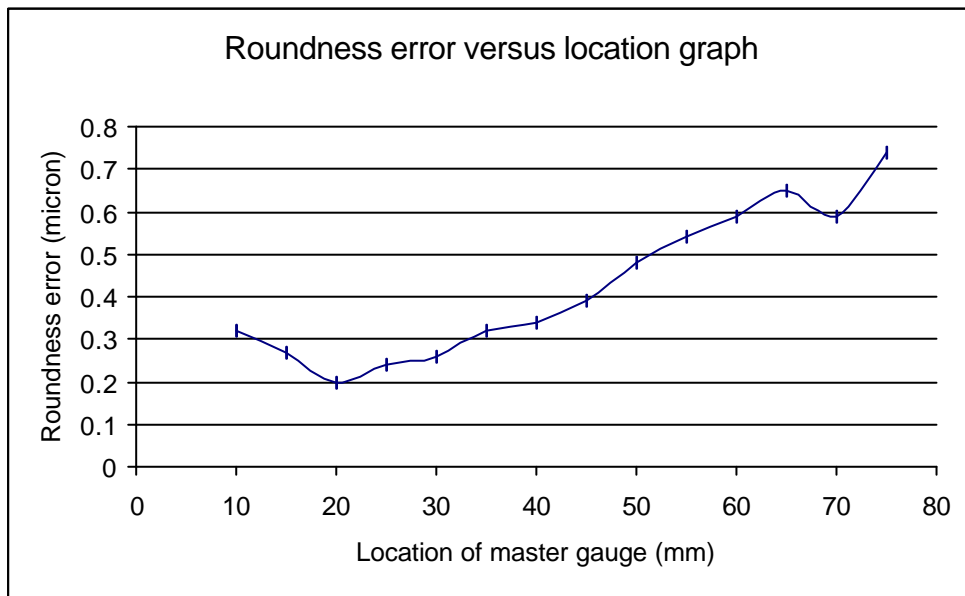


Figure 3.8 Roundness error of master gauge along the length

Aeroel Slit laser measurement of master gauge

Location of measurement from chuck (mm)	Diameter (mm)	Variation (micrometer)
10	40.0043	0
15	40.0041	-0.2
20	40.0043	0
25	40.0042	-0.1
30	40.0044	0.1
35	40.0052	0.9
40	40.0071	2.8
45	40.0073	3
50	40.0058	1.5
55	40.0052	0.9
60	40.0047	0.4
65	40.0046	0.3
70	40.0048	0.5
75	40.0063	2

Table 3.2 Diameter measurements of master gauge

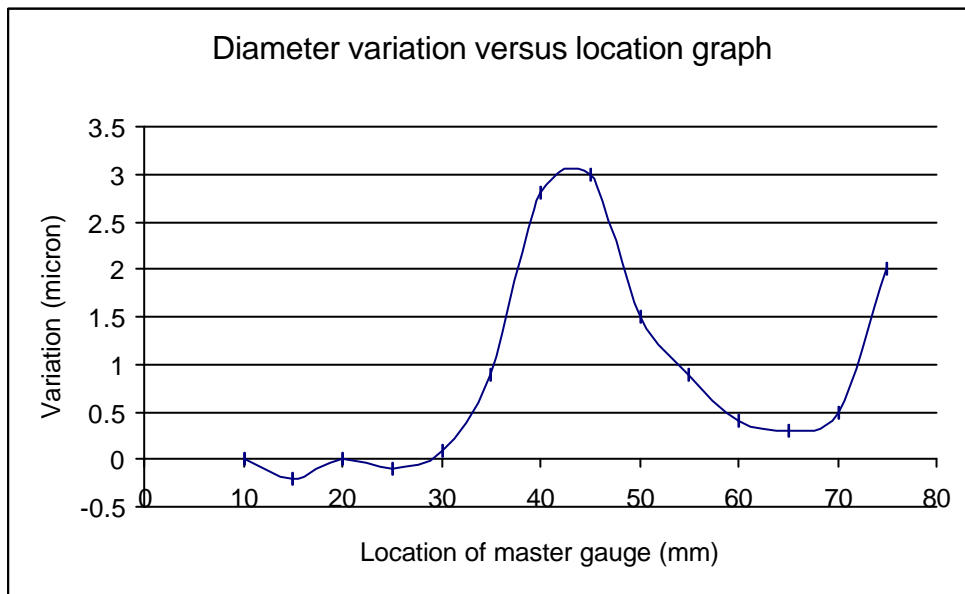


Figure 3.9 Diameter variation of master gauge along the length

3. 3. 2. Measurement of cylindrical master gauge on the chuck of CNC machine (lapped)

Cylindrical master gauge is measured in CNC machine on the chuck by using *Keyence LK 2001* laser displacement sensor, which has 1-micrometer resolution, 30 mm operating distance and 2000 Hertz sampling frequency (Figure 3.10)[11].

National Instruments Labview 6.i signal processing software with its hardware is used for laser displacement sensor and thermocouple reading.

Two basic measurements were performed on CNC turning machine. These are linear and rotating measurements. These measurements are performed in order to find the linearity error of axis of CNC machine, and basic set-up errors (eccentricity, tilting).

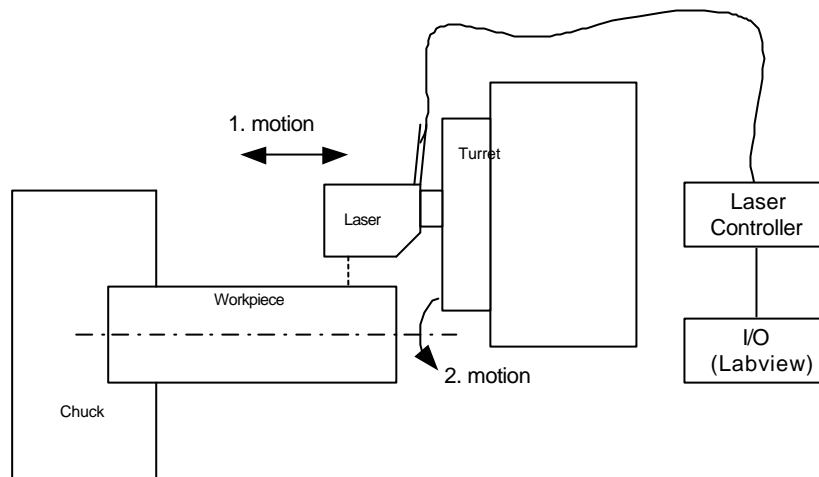


Figure 3.10 In process measurement in CNC Lathe

3.3.2.1. Linear measurements

Linear measurements are performed for 12 positions (0,30,...330) of the workpiece. At each position linear measurements were performed from end face of part to the chuck position (totally 50 mm feed motion of CNC machine). The figure 3.11 shows the measurement technique used for linear measurements.

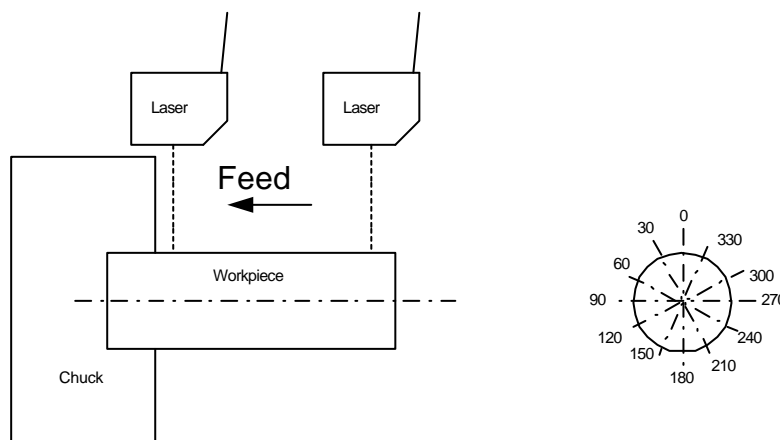


Figure 3.11 Linear measurements

In linear measurements, three basic errors are encountered. These are straightness of workpiece, straightness of CNC x-axis guide, and tilting (wobbling) error of workpiece clamping to the chuck. The former can be neglected because of specification of perfect lapping gauge. This gauge has less than 1.5-micrometer straightness error. So, the other two contributes to the error measured by the laser. The measurement results are given in table 3.3;

Location of measurement (deg)	1. Experiment (error)(μm)	2. Experiment (error) (μm)	3. Experiment (error) (μm)	4. Experiment (error) (μm)
0	35	31	62	60
30	44	38	74	61
60	55	49	80	35
90	59	57	73	19
120	59	57	58	14
150	53	45	43	15
180	44	45	32	28
210	38	33	27	43
240	28	28	26	38
270	26	24	28	54
300	29	25	36	63
330	31	28	46	60

Table 3.3 Linear measurements of master gauge in CNC machine

The results show that all errors are positive from the end of the part to the one of the chuck. The *MS Excel* figure shows the first experiment results at different angle locations. In all locations, the distance from laser to the workpiece at the end position is decreasing towards the chuck. The only difference is the rate of the decrease at different measurement location. This is due to the wobbling (tilting) error dependence on location. The important result that can be shown is the comparison of the magnitude of the straightness error to that of tilting (wobbling error). In all measurements, straightness error due to guides is higher than wobbling error in all measurement locations (Figure 3.12).

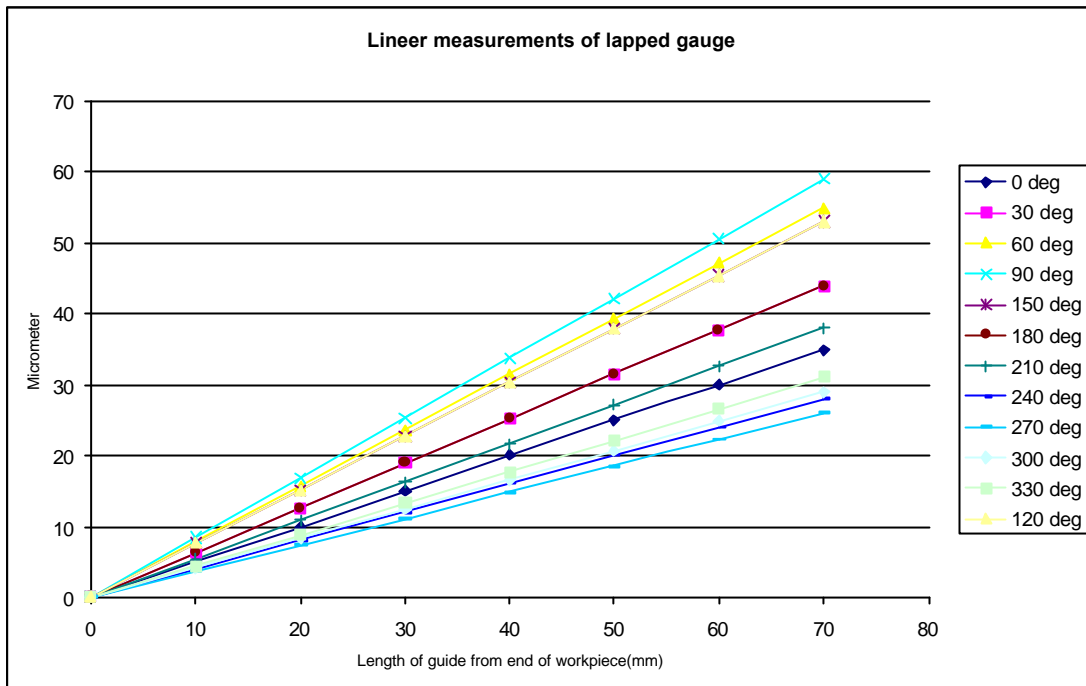


Figure 3.12 Laser measurements with respect to chuck end position

If the measurement results are plotted with respect to measurement locations, approximately a sinusoidal curve is seen. This is due to the changing of tilting (wobbling) error of workpiece with respect to measurement location. Since the wobbling (tilting) error is changing sinusoidally along the rotation of spindle, straightness error of guide is constant over rotation of the spindle. This is proved by the results shown above. In table 3.3 these are the two values in each column. These are max and min values of the experiments:

Experiment 1: max: 59 μm 90° location min: 26 μm 270° location

Experiment 2: max: 57 μm 90° location min: 24 μm 270° location

Experiment 3: max: 80 μm 60° location min: 26 μm 240° location

Experiment 4: max: 63 μm 300° location min: 14 μm 120° location

It is easy to conclude that max and min values are 180 degree apart from each other. This is the nature of wobbling (tilting) error (Figure 3.13a, 3.13b, 3.14).

wobblemax)

3-16

$\text{Error}_{\min} = \text{Straightness error} - \text{Tilting max}$ ($\epsilon = \epsilon_{\text{wobblemin}} = \epsilon_{\text{wobblemax}} + \delta$)

3-17

So ;

$$\text{Straightness of guide of CNC machine} = \frac{\text{Error}_{maz} + \text{Error}_{min}}{2} \quad 3-18$$

Also;

$$\text{Maximum tilting error} = \frac{\text{Error}_{maz} - \text{Error}_{min}}{2} \quad 3-19$$

So;

Result are given in table 3.4

Experiment	Straightness error of guide	Maximum wobbling error
1	43	17
2	41	17
3	49	21
4	40	24

Table 3.4 Results of rotational measurements of master gauge in CNC machine

It can be concluded for linear measurement that **straightness of CNC machine is approximately 40 μ m/50 mm**. Maximum wobbling is dependent on chuck clamping of workpiece and has no effect on dimensional error.

Compensation of CNC Guide straightness error

The straightness error 0.8 μ m/mm (40 μ m/50mm) could be compensated by parameter setting of CNC software. But this machine control software (*GE Fanuc 21*) has no such parameter setting. So straightness error is compensated in the G-code part program. Below shows the G-code program with its explanation written in CNC program [18]. But this is not effective method for this compensation, as it results in steps on the surface (3 μ m). The table below shows the diametrical variation of workpiece with compensated and uncompensated results by using *Aeroel Slit laser*. In compensated cutting, the total reverse straightness error over 50mm (38 μ m/50 mm) was fed to the program. Location of measurement is given from one end of the workpiece to the other end of the workpiece clamped on the chuck (Table 3.5)(Figure 3.15, 3.16a, 3.16b).

Location of measurement	Diameter(mm) Uncompensated	Diameter(mm) Compensated	Variation(\hat{i} m) Uncompensated	Variation(\hat{i} m) Compensated
0mm	41.9261	41.7428	0	0
5mm	41.9209	41.7405	-5.2	-2.3
10mm	41.9173	41.7411	-8.8	-1.7
15mm	41.9141	41.7433	-12	0.5
20mm	41.9096	41.7423	-16.5	-0.5
25mm	41.9059	41.7408	-20.2	-2
30mm	41.9016	41.7426	-24.5	-0.2
35mm	41.9002	41.7421	-25.9	-0.7
40mm	41.8960	41.7421	-30.1	-0.7
45mm	41.8923	41.7424	-33.8	-0.4

Table 3.5 Comparison of diameter measurements of workpiece between compensated and uncompensated case

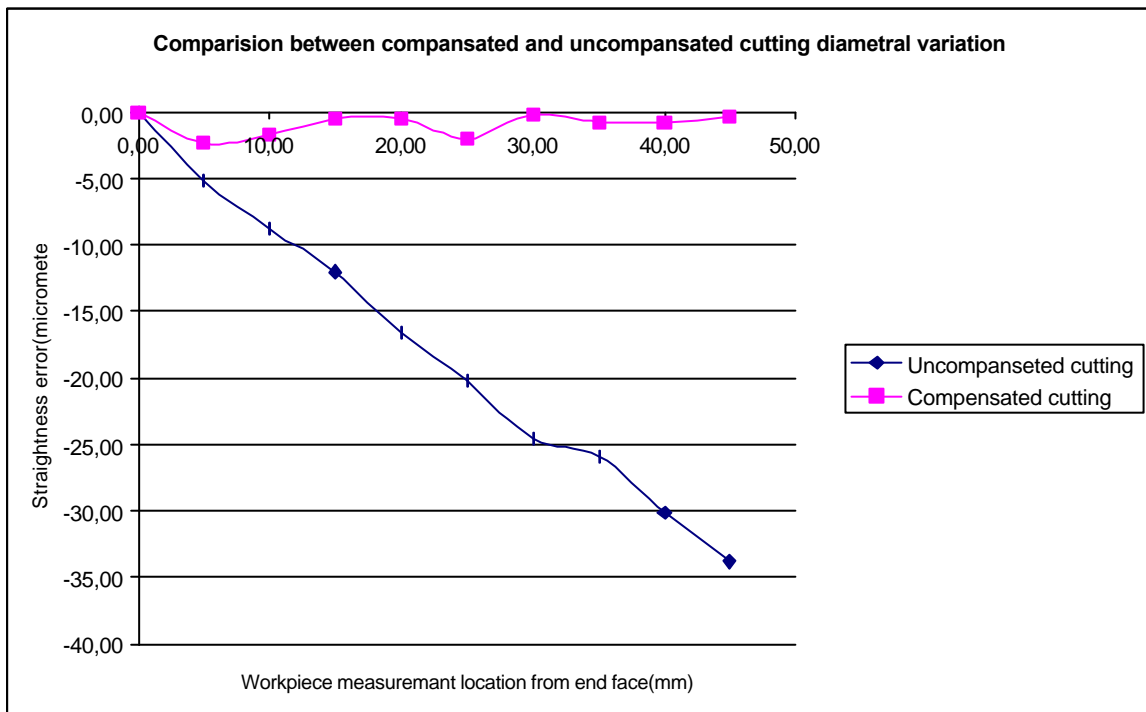


Figure 3.15 Comparison between compensated and uncompensated cutting case

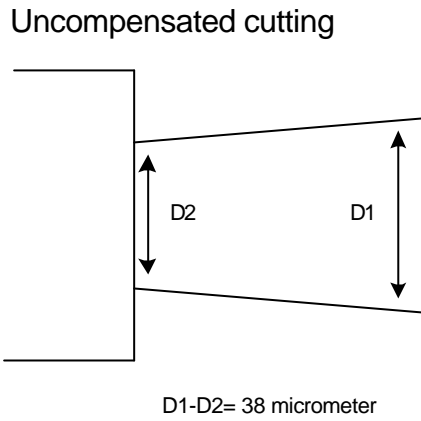


Figure 3.16a Uncompensated cutting

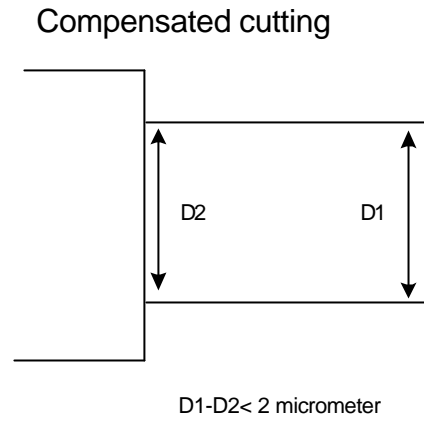


Figure 3.16b Compensated cutting

3. 3. 2. 2. Rotating measurements:

Rotating measurements are performed for different sections of the workpiece (25,30,70mm away from starting point of chuck). At each position, rotational measurements were taken both manually and CNC spindle motion. The figure 3.17 below shows the measurement technique used for rotational measurements.

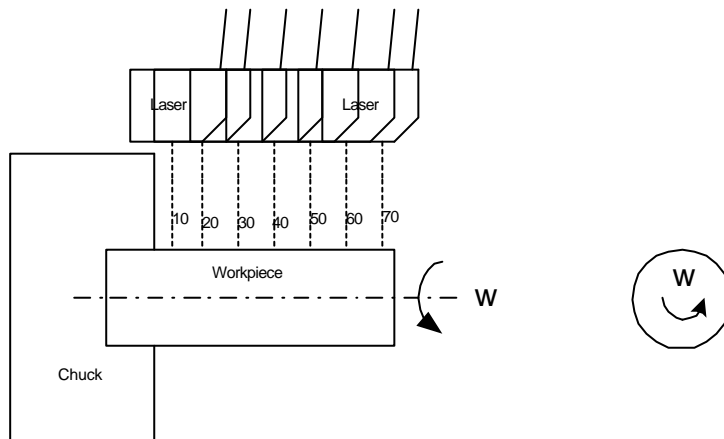


Figure 3.17 Rotational measurements

Because of inaccuracy of operator hand to rotate the spindle, CNC spindle motion is preferred. But this motion has limited minimum angular velocity. This is 150 rpm.

So;

$$\text{Spindle frequency} = 150/60 = 2.5 \text{ Hertz}$$

$$\text{Laser frequency} = 2000 \text{ Hertz}$$

position. But some figures increases and some decreases with increasing length from the chuck. This is because of the nature of tilting (wobbling) error. In 1,2 and 3

experiments, wobbling error decreases the overall error of the workpiece along the length as it can be seen in the figure. Rotational error at the chuck position can be assumed as the centering error. Since it depends on the clamping conditions in the chuck, it changes from experiment to experiment. But overall, 45-50 μm centering error is seen on the measurement for different clamping.

From rotational measurements two important errors (tilting and centering) are set-up errors. These errors do not affect the dimension during cutting. The reason for this is given in section 2 (Effect of centering on dimension in cutting).

Effect of CNC x-axis guide's side linearity on measurement

It was found that CNC x-axis guide straightness error in z (normal to workpiece) direction is nearly 40 μm . It would be assumed that this guide would have more or less same straightness error in side (tangential to workpiece) direction, because the axes of CNC turning machines have same properties. So, how would this error affect the accuracy of laser measurement? The figure below shows the measurement error on workpiece (Figure 3.19).

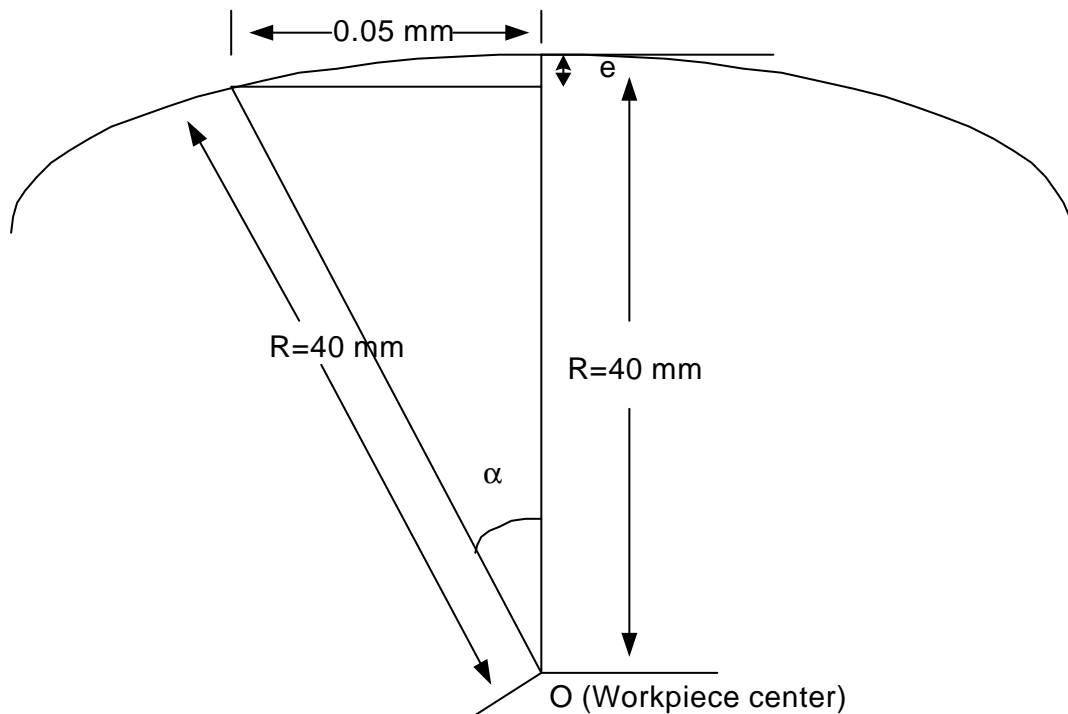


Figure 3.19 Effect of side straightness on measurement

Maximum 50 μm straightness error;

$$\tan^{-1}(\mathbf{a}) = \frac{0.05}{R} = \frac{0.05}{40} = 0.0716 \text{ deg.}$$

$$R \cdot \cos(\mathbf{a}) = 40 \cdot \cos(0.0716) = 39.99997 \text{ deg.}$$

$$\text{Error} = e = R - R \cdot \cos(\mathbf{a}) = 40 - 39.999969.$$

$\text{Error} = e = 0.031 \text{ } \mu\text{m}$. It is so negligible with respect to resolution of laser.

In this chapter, analysing the errors of workpiece, sources of the errors and possible compensation techniques were examined in detail. In order to characterise the CNC lathe, some experimental studies were performed by using some tools (National Instruments Labview 6.i signal processing software and I/O card, laser displacement sensor, thermocouple, Aeroel slit laser, Roundness measuring machine).

It can be concluded in this chapter that, CNC turning machine axis error is 40 μm and this error is eliminated in the G-code part program. The set-up errors (eccentricity, tilting) are on the order of 50-90 μm . But these errors do not contribute geometric error on the workpiece after cutting.

CHAPTER 4

DEVELOPMENT OF THE SYSTEM (PBCD)

In this chapter, design of PBCD and its components are explained in detail. These components are piezo stack actuator, piezo stack actuator's voltage amplifier, mechanical housing, tool tip, piezo sensor amplifier circuit, dSPACE 1102 hardware and software, Simulink software and CNC turning machine spindle motor encoder. First, these components are described and then the assembly of PBCD is explained. The figures of PBCD components are given in Appendix.

4. 1. Piezo stack actuators

Piezo stack actuators are separately contacted layers of ceramics, which introduce motion when a voltage difference or electric field is applied. This motion is due to the inverse piezoelectric effect. Usually the cross section of piezo stack actuators is circular or rectangular.

Main application areas of piezo stack actuators are precise positioning for one or multi axis stages, mirrors in optics, micro robots and active vibration control.

Characteristics of piezo stack actuators

Piezo stack actuators have some critical properties, which are essential in many applications. Hysteresis, creep, stroke, stiffness, resonant frequency, electrical capacitance and power consumption should be considered while choosing the piezo stack actuators. In this chapter, these properties are measured experimentally by using measuring instruments (*Mitutoyo Roundtest RA-114, Agilent 35670A Dynamic signal analyzer*).

4. 1. 1. Hysteresis

Hysteresis, being an unwanted nonlinear behavior of piezo stack actuators, is defined as the maximum difference between the up going and down going output values in a sequential operation of piezoelectric actuators. Usually the cause of the hysteresis is dependent on previous output values of piezoelectric actuators. Hysteresis of piezoelectric actuators is due to the crystalline polarization effect and

friction in molecular base. The piezo stack actuator open loop output motion is dependent not only the current input value but also on previous inputs. Hysteresis of piezo stack actuator is found experimentally. The figure 4.1 shows the measured hysteresis curve of piezo stack actuators. Hysteresis curve is plotted by giving approximately 30 Volt increments or decrements from piezo stack amplifier. The tests are performed with *Mitutoyo Roundtest RA-114 Inductive contact probe*, which has 10nm resolution and $\pm 1\text{mm}$ range [12].

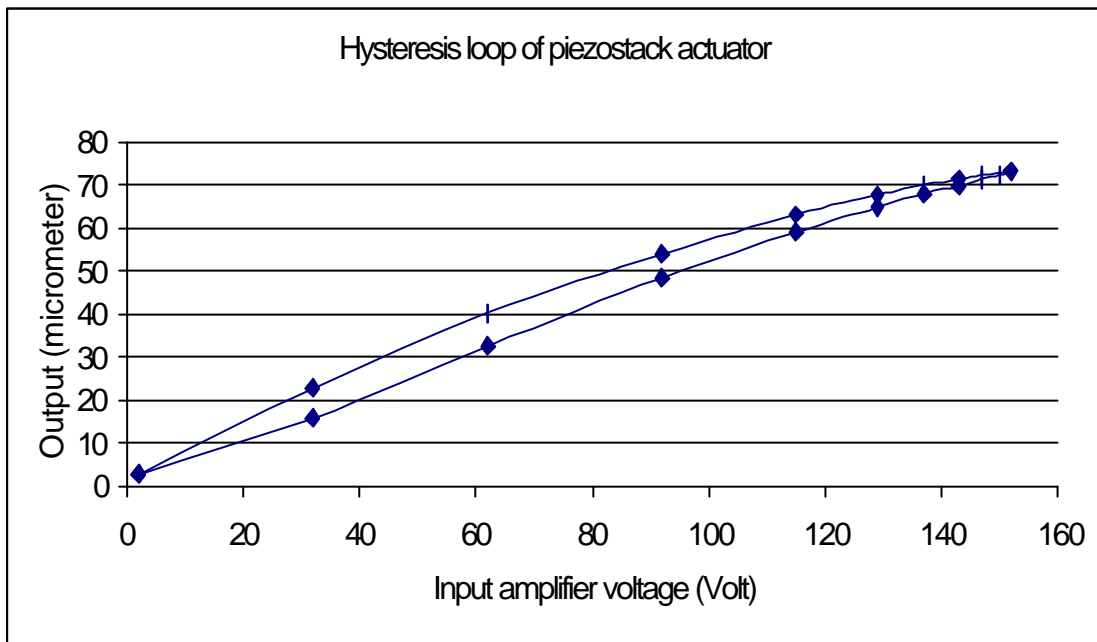


Figure 4.1 Hysteresis loop of piezo stack actuator

Hysteresis can be eliminated by closed loop control.

4. 1. 2. Creep (Drift)

Creep is the time dependent change of output (motion) of piezo stack actuator. Like hysteresis, it is one of the major limitations of piezo stack actuators. Creep decreases logarithmically with time. It is the slow output response after change in input is completed. The following equation describes the creep of piezo stack actuators [13].

$$\Delta L(t) \approx \Delta L \cdot (1 + g \cdot \lg \cdot (\frac{t}{0.1})) \quad 4-1$$

Where,

ΔL is displacement 0.1 seconds after the voltage change is completed.

γ is creep factor which is dependent on the properties of the actuator

t is time

Creep of open loop piezo stack actuator is measured and plotted below in figure 4.2.

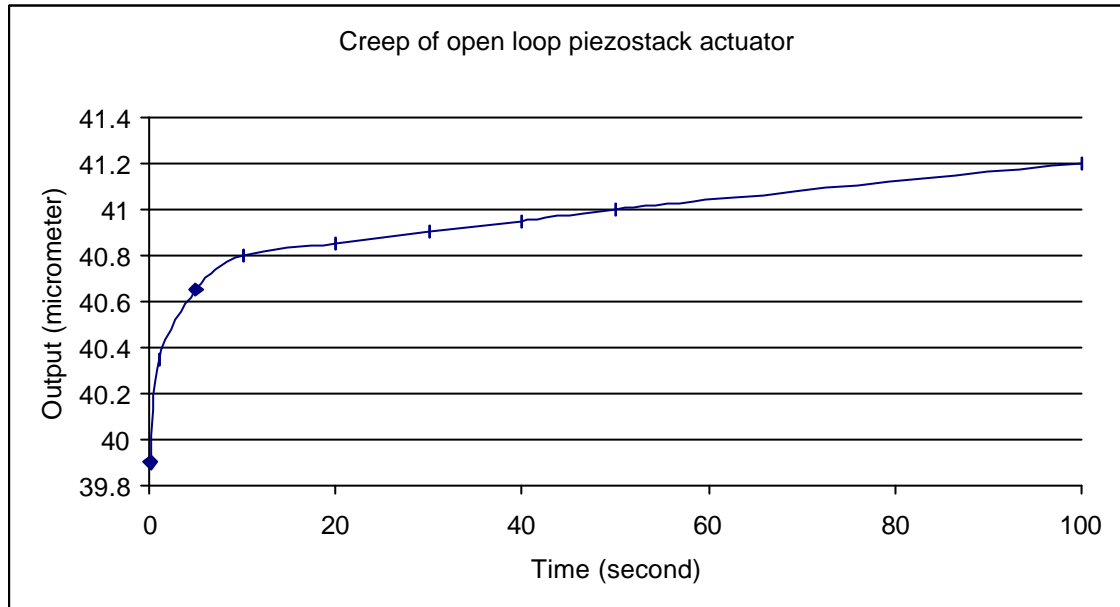


Figure 4.2 Creep of open loop piezo stack actuator

Like hysteresis, creep can be eliminated in closed loop control of piezo stack actuators.

4. 1. 3. Stroke

Piezo stack actuator that is used for PBCD can be operated at bipolar voltage input values. Its input voltage is between -30Volt to 150Volt . The maximum stroke, which is the response to the mentioned input voltage values, is $105\ \mu\text{m}$. However, in PBCD applications, only unipolar inputs are used in experiments. So the maximum stroke for unipolar inputs, which is from 0Volt to $150\ \text{Volt}$, is $80\ \mu\text{m}$ [14].

4. 1. 4. Stiffness

Stiffness is the elastic property of piezo stack actuators. It shows how much deformation is detected when a force is applied. Stiffness of piezo stack actuator used

in PBCD is $6\text{N}/\mu\text{m}$. If full stroke of motion, i.e. $105\mu\text{m}$, is needed, $105 \cdot 6 = 630\text{N}$ force is required.

Stiffness of PBCD is different from piezo stack actuator. PBCD is stiffer than piezo stack actuator.

4. 1. 5. Resonant frequency

Piezo stack actuators have generally higher resonant frequencies. Resonant frequency of piezo stack actuator used in PBCD is 12 kHz. But the resonant frequency of the unloaded actuator is not important. Because any external mechanical component or mass reduces the resonant frequency of the system.

4. 1. 6. Electrical Capacitance

When operated well below the resonant frequency, piezo stack actuator behaves as a capacitor. Since the displacement is directly proportional to charge or voltage applied on piezo stack actuator [14]. The capacitance of the piezo stack actuator used in this research is 3200 nF.

4. 1. 7. Power consumption

A typical piezoelectric actuator dissipates only small amount of power (order of milliwatts), which will not affect thermal equilibrium of a precision machine. On the other hand, equivalent electromagnetic actuators dissipate much more power due to the winding resistances and eddy current losses [36].

4. 2. Piezo voltage amplifier

In order to operate the piezo stack actuator, appropriate piezo voltage amplifier is required. Piezo stack amplifiers amplify the input signal in sufficient voltage level necessary to move the actuator.

4. 2. 1. Specifications of piezo voltage amplifier

Specifications of piezo voltage amplifier used in this research are tabulated below:

Voltage range	: -30 Volt through 150 Volt
Gain factor	: 30

Max./average current : 60 mA
 Bandwidth : 20 kHz
 Number of channel : 1

4. 2. 2. Limitations of piezo voltage amplifier

The maximum/average current value of the piezo voltage amplifier limits the piezo stack actuators dynamic operation. Actually producer specifies this limit. Because overheating of piezo stack actuators is becoming a problem at high frequencies. There is a loss of energy during charging and discharging. The loss of energy is due to heat dissipation.

Since from a well known equation

$$I = C \cdot \frac{dV}{dt} \quad 4-2$$

Where

I is current of piezo voltage amplifier

C is electrical capacitance value of piezo stack actuator

$\frac{dV}{dt}$ is voltage change per unit time

This equation can be rewritten for sinusoidal input of piezo stack actuators as follows:

Average current

$$I_{ave} = C \cdot V \cdot f \quad 4-3$$

Maximum current

$$I_{max} = 2 \cdot \mathbf{P} \cdot C \cdot V \cdot f \quad 4-4$$

Where

f is frequency of piezo stack actuator

V is amplitude of input voltage

Using above equations, maximum frequency at which piezo stack actuators can be operated is found. For example; for full stroke

$$I_{\max} = 60mA, C = 3200nF, V = 150V$$

Maximum frequency that piezo amplifier can give: 19.894 Hertz

The table 4.1 shows the amplitude and frequency couple of piezo stack actuators under maximum piezo voltage amplifier current.

Maximum current (mA)	Voltage amplitude (Volt)	Displacement (μm)	Frequency (Hertz)
60	150	80.0	19.9
60	100	53.3	29.8
60	10	5.3	298.4
60	1	0.5	2984.1

Table 4.1 Amplitude and frequency couple of piezo stack actuators at maximum piezo voltage amplifier current

4. 3. Piezo sensor amplifier circuit

Piezo stack actuators used in this thesis have two cables, which are power supply and feedback output. The feedback cable has three small cables in it. Those cables have different colors, which are shown in the figure 4.3 with the amplifier circuit. There are two strain gauges that have 5-milivolt voltage differences between them and with these cables they constitute half Wheatstone bridge circuit. In order to make full Wheatstone bridge circuit, two resistors are connected to these cables. Wheatstone bridge circuit provides a means for accurately measuring resistance and for detecting small changes in resistance. In the figure 4.4 below R_1 is a strain gauge that experiences a change in resistance with a change in the displacement of piezo stack actuator. Change in one strain gauge gives the feedback that is proportional to the displacement of piezo stack actuator [15].

In the circuit, an amplifier 17741 integrated circuit (IC) was used to increase the change of voltage difference. In this circuit, amplifier factor is 1000. So the voltage difference was amplified by 1000 times $(R_2/R_1)=1000$. The aim of using this amplifier is increasing the resolution of the controller. Both Wheatstone bridge and amplifier IC (Integrated Circuit) are fed by power supply. Full amplifier and Wheatstone bridge circuits are shown in the following figures 4.3, 4.4.

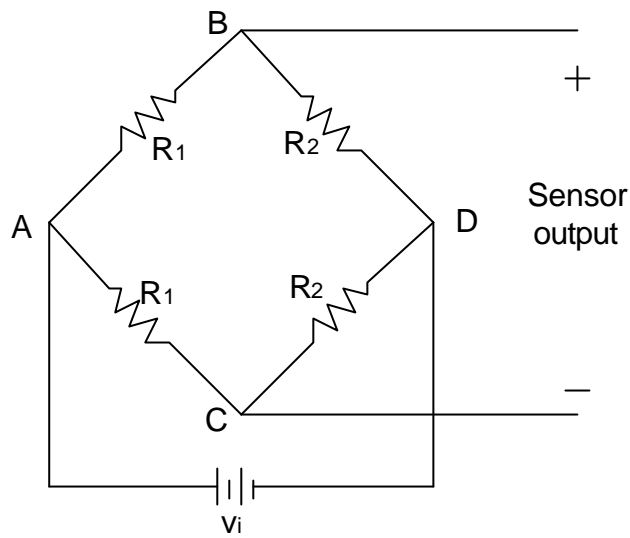


Figure 4.3 Wheatstone bridge circuit

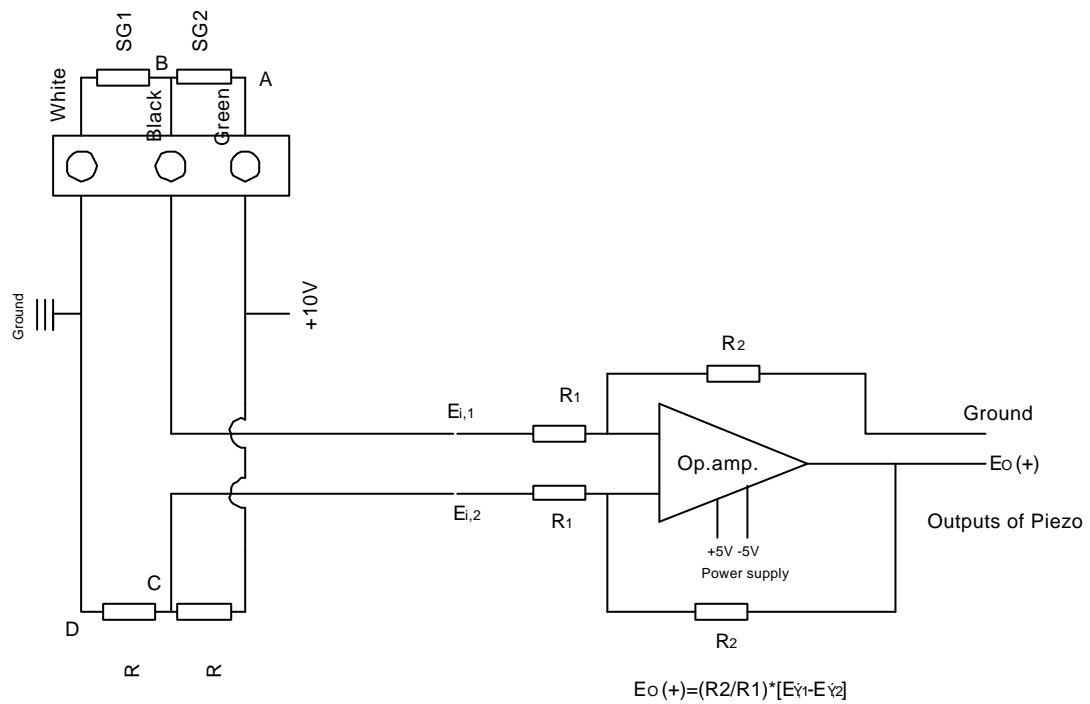


Figure 4.4 Amplifier circuit for piezo feedback

4. 4. Tool tip

The tool tip is made up of the standard tool holder that is cut to match proper dimension for the design of PBCD. The model of tool holder is SDJCL 1212F 07 (12mm X 12mm, Left oriented). The mechanical drawing of the tool tip cut is given in the appendix.

The tool insert used in this research is *PLANSEE TIZIT 10 HM-WENDEPLATTEN*.

4. 5. Mechanical housing

The design of piezo stack actuator mechanical housing is based on the simple flexure lever amplifier system. The main disadvantage that affects the design is the limitations of the turret tool holder fold space. The principle of the housing design is the deflection of the housing tip. The simple figure of the piezo and housing tip is shown in figure 4.5:

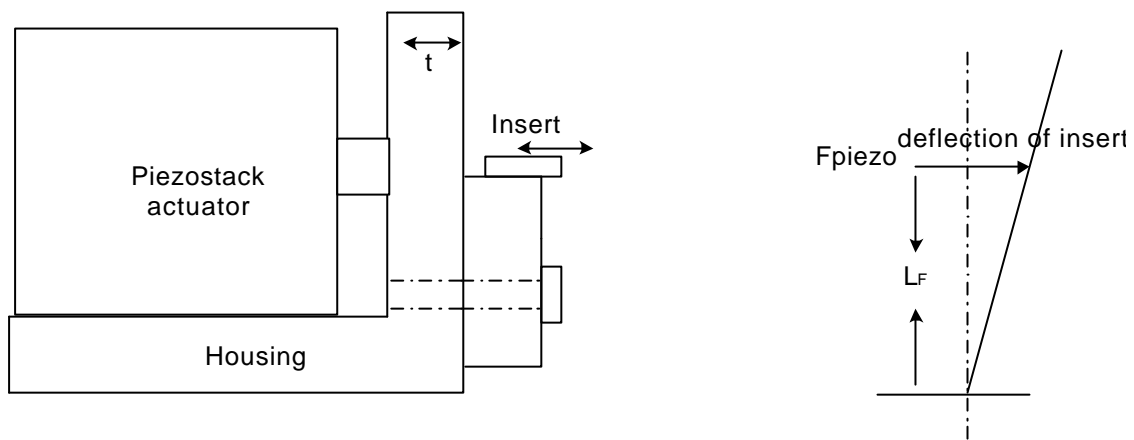


Figure 4.5 Piezo housing

Mechanical drawing with its dimension is given in the appendix. FEA (Finite Element Analysis) is performed for deflection and force analysis. Deformation and Von-Misses analysis are given in the appendix. The important result is the maximum displacement that is the output of 0-150 Volt piezo voltage amplifier input of the PBCD. Approximately 23 μm displacement is observed from the FEA of the PBCD. FEA is performed at *Catia V.5* Software. In the real case, the measurement results of PBCD show good similarity with FEA. Inductive probe, which is on the Mitutoyo Roundtest, RA-116, is used to measure the real displacement of the PBCD. The result of the real displacement of the PBCD is shown in the figure 4.6.

$$\Delta x = \frac{F_s}{k_t} \quad 4-5$$

Where

F_s is force exerted on PBCD by piezo stack actuator

k_t is stiffness of housing at the insert location

stack actuator side by

$$\Delta x = S - \mathbf{d}_p \quad 4-6$$

Where

S is displacement of piezo stack actuator

\mathbf{d}_p is deflection of piezo stack actuator.

Deflection of piezo stack actuator can be found by stiffness of piezo stack actuator (k_p) and force exerted on PBCD by piezo stack actuator (F_s).

Then,

$$\Delta x = S - \frac{F_s}{k_p} \quad 4-7$$

Combining the equations (4-6) and (4-7)

$$\Delta x = S - \left(k_t \cdot \frac{\Delta x}{k_p}\right) \quad 4-8a$$

$$\Delta x = \frac{S}{1 + \frac{k_t}{k_p}} \quad 4-8b$$

Since k_p is $6\text{N}/(\mu\text{m})$ and k_t is found $15\text{N}/(\mu\text{m})$,

$$\Delta x = \frac{S}{1 + \frac{15}{6}}$$

$$\Delta x = \frac{S}{3.5}$$

So the displacement of the PBCD is reduced by 71.43 %.

If S were a full stroke of piezo stack actuator,

$$\Delta x = 80\mu\text{m} / 3.5 = 22.8\ \mu\text{m}.$$

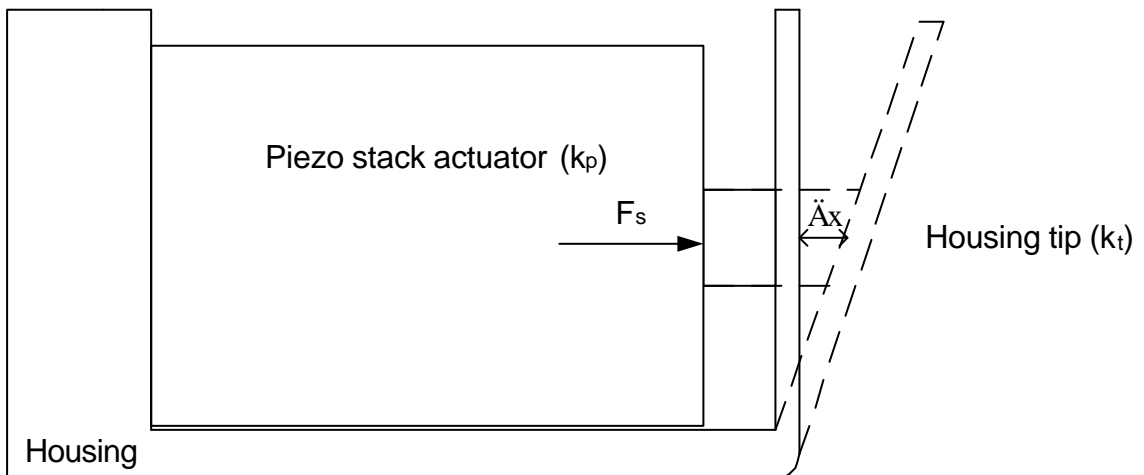


Figure 4.7 Principle of piezo housing

Therefore, the mechanical housing reduces the full stroke of the system from 80 mm to 23 mm.

4. 6. dSPACE 1102 hardware and software

Dspace 1102 software and hardware are used with Matlab to run Simulink simulations in real time for PBCD. Piezo stack voltage amplifier and piezo stack actuator feedback data are connected to the dSPACE 1102 card. Also CNC turning machine spindle motor encoder data is fed to the controller for dynamic operation of piezo stack actuator. So one D/A (digital to analog) converter for analog voltage amplifier, one A/D (analog to digital) converter for feedback of piezo stack actuator, and one encoder reading are connected.

4. 7. P. C.

CPU : Pentium 733 MHz
RAM : 128 MB
Operating system : Windows 98

4. 8. CNC Turning machine

The PBCD is mounted on the EMCO 155 PC Turn machine (Figure 4.7). Specification of this machine is given below:

Spindle

Spindle motor : step
Spindle motor encoder : 1024 ppr
Spindle motor speed : 150-4000rpm

Axes

Feed motor : Step
Step resolution : 1.25µm
Slide traverse : X: 100mm, Z:300 mm
Control : Fanuc 21



Figure 4.8 EMCO 155 PC Turn machine

CHAPTER 5

EXPERIMENTS AND RESULTS

5.1. Control of piezo stack actuator

PID (Proportional Integral Derivative) control, which more than half of the industrial controller use, is implemented for PBCD control. The applicability of the PID control to most control systems makes it very useful and popular for all controllers. Especially for systems where the analytical design methods can not be implemented because of the unknown model of the systems. Like these systems PBCD mathematical model is not known. Figure 5.1 shows the PID control of a plant.

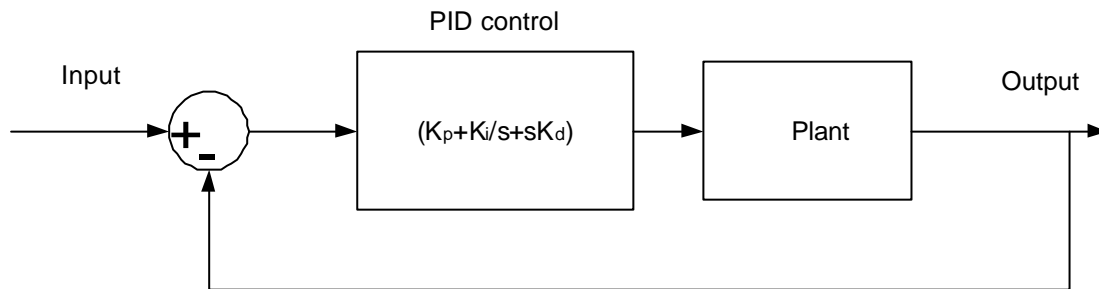


Figure 5.1 PID control

The requirement of the control is to compensate the nonlinear behavior (hysteresis and creep) of piezo. In order to find optimum parameters of the controller, Ziegler-Nichols' second rule is used.

Ziegler-Nichols Rule

The process of selecting the controller parameters to provide the given performance specification is known as controller tuning. For PID parameters tuning, Ziegler-Nichols suggested a rule to set K_p , K_i , K_d based on some experiments. These experiments are known as Ziegler-Nichols first and second method. In the first method, the plant's response to unit-step input is examined. If the response looks like S-shaped, this method works. This S-shaped curve is characterised by two parameters, which are response delay time and time constant. These parameters can be found by simply drawing a tangent line at the turning point of the S-shaped curve. If the first

method does not work, the Ziegler-Nichols second rule is used. Second method is based on the response of the plant to the proportional control action. Starting from zero value of K_p up to the critical value, oscillations are looked for. At this critical value, the period $T_{critical}$ of this oscillation is determined. Both $K_{p,critical}$ and period $T_{critical}$ are used in the calculation of PID parameters in the following table 5.1 [16].

K_p	K_i	K_d
$0.6 \cdot K_{p,critical}$	$\frac{0.6 \cdot K_{p,critical}}{0.5 \cdot T_{critical}}$	$0.6 \cdot K_{p,critical} \cdot 0.125 \cdot T_{critical}$

Table 5.1 Calculation of PID parameters by using Ziegler-Nichols first method

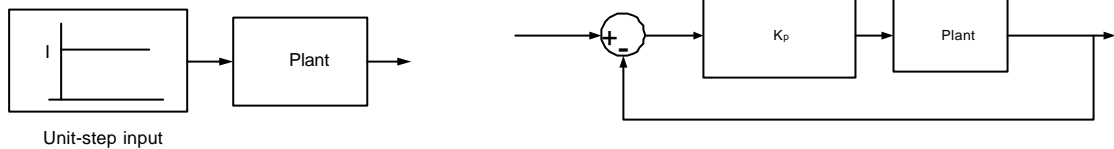


Figure 5.2a Ziegler-Nichols first method Figure 5.2b Ziegler-Nichols second method

Ziegler-Nichols' first method is applied to the PBCD (Figure 5.2a). But the S-shaped curve is not seen. So this method is not applicable for PBCD. On the other hand, the second rule works on PBCD (Figure 5.2b). The parameters of the PID are tabulated below according to the table above and, which is applied to the second method of Ziegler-Nichols. After applying this method $K_{p,critical}$ and $T_{critical}$ are found 1.73 and 0.04878 respectively. The corresponding PID parameters are tabulated in Table 5.2. These PID parameters are tuned while observing the performance of the dynamic position control of PBCD. So K_p and K_i are increased according to the response of the system.

K_p	K_i	K_d
1.04	42.64	0.024

Table 5.2 PID parameters of PBCD control

5. 2. Constant position control of PBCD

Constant position control is the control algorithm written in dSPACE software. In this control, a constant step value is given to the PBCD. The main purpose of this control is to keep the PBCD tool tip constant during the cutting operation. So that, by using this control the PBCD deflection is eliminated during cutting. Since the cutting forces deflect the tool in the cutting operation, the tool position would not be constant in the cutting operation. The constant position control would be very effective to keep the PBCD tip in the cutting position like highly rigid tools that have very small deflection.

In constant position control of PBCD the surface characterisation changes, after cutting with zero constant displacement input command of PBCD, are investigated. The corresponding Simulink program is given in the appendix. In the program, the constant command is multiplied by displacement gain in order to get the command at the feedback voltage level. This displacement gain is found to be 0.23. Actually, this value means that 1 μm position gives 0.23-Volt feedback. After the feedback data is subtracted from the command, error is obtained. In fact, multiplying error with error gain gives position error. The error gain is 4.35 that is the inverse of displacement gain. Added PID (K_p , K_i , K_d) parameters multiplied by the error is normalised for dSPACE to put it into the acceptable range. The PID parameters are as follows: $K_p = 42.04$, $K_i = 2000$, $K_d = 0.024$. PID parameters are found from Ziegler-Nichols method and tuning. The normalisation value (control gain) is found as 0.03. The control output found after control gain is sent to D/A converter for piezo voltage amplifier to supply voltage to piezo stack actuator. A/D converter takes feedback coming from feedback amplifier circuit. After multiplying by 10, which is the Simulink gain, data is normalised by adding feedback normalisation value. Table and figure 5.3 show the feedback value for corresponding displacement of piezo stack actuator. With the help of this table, feedback normalisation is found $5.25\text{Volt} / (5.7+16.2)\mu\text{m} = 0.23\text{V}/\mu\text{m}$. Also the feedback is multiplied by -1 after adding feedback normalisation to get final ordered feedback signal. Since the signal is very noisy, a low pass filter is added before subtracting from the input command. The filter Chebyshev I with low pass cut-off frequency of 1 rad/sec (0.16 Hz), and order of filter one is used. Since the PBCD is implemented by constant position control, cut-off frequency is chosen so small. Therefore filtering eliminates nearly all of the noises.

On the other hand, the main drawback of using this filter is the increase of response time. Because of the low filter cut-off frequency, the response becomes very slow. The sampling period of constant position control of PBCD is found 35 μ sec.

Displacement of PBCD (μ m)	Feedback of piezo (Volt)	Feedback after normalisation (Volt)
-5.7	8.5	0
-3.8	8.1	0.4
-1.85	7.65	0.85
0.15	7.2	1.3
2.15	6.72	1.78
4.2	6.23	2.27
6.3	5.77	2.73
8.3	5.23	3.27
10.35	4.78	3.72
12.3	4.24	4.26
14.3	3.78	4.72
16.2	3.25	5.25

Table 5.3 Feedback normalisation of PBCD

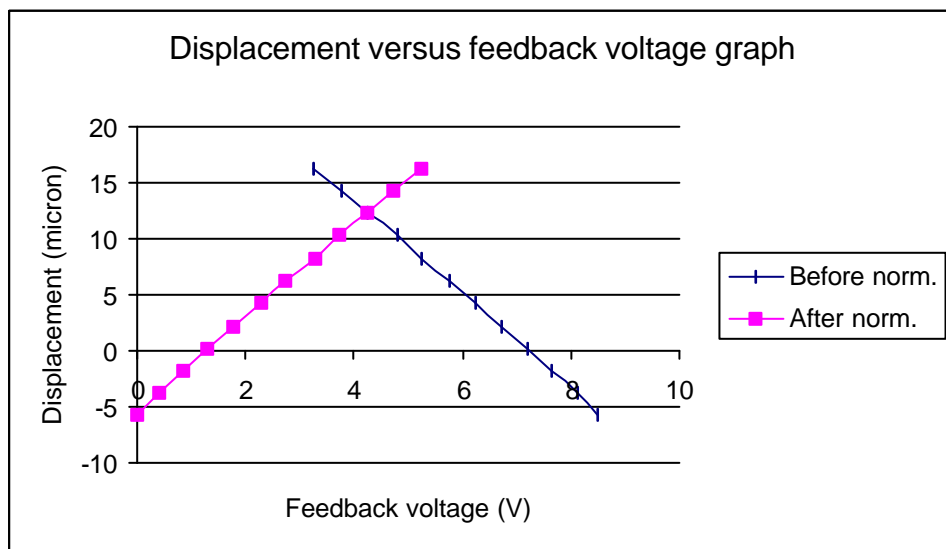


Figure 5.3 Feedback normalisation of PBCD

PBCD is ready for cutting operation in CNC machine after constant position control, which is explained above (Figure 5.4). The results on the surface after cutting with constant position control of PBCD are compared with non-controlled PBCD cutting operation. Same Gcode program is used as in the straightness of the CNC machine. The surface of workpiece is measured at roundness measuring machine (*Mitutoyo Roundtest, RA-116*). The measurements of the cross-section locations are also given in the table. The tables show that, at least 20-30 % of improvement is achieved after applying constant position control of PBCD. This improvement is explained as the better control of PBCD to overcome the deflection of tool workpiece couple than no control application of PBCD. There are four examples for different cutting conditions. The polar graphs of these examples are given in the Appendix. Examples are shown below (Example 1,2,3 and 4).

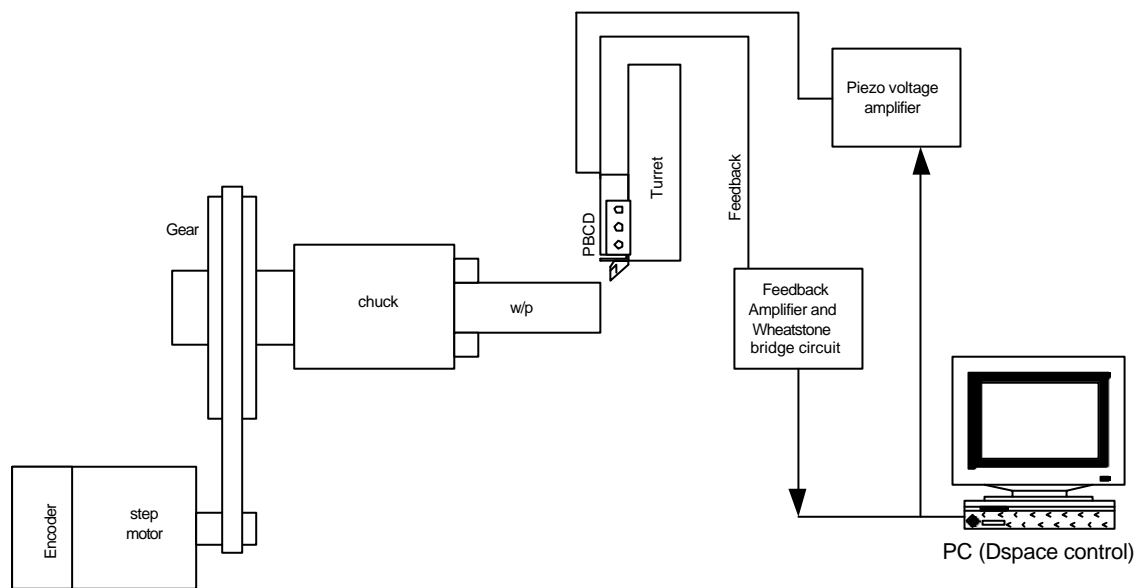


Figure 5.4 Constant position control of PBCD

Example 1

In this example, the performance of the PBCD under constant position control with respect to no control is investigated. Differences in the errors of both cases and improvements of the surface error on workpiece are found. The PBCD is used in the cutting in CNC turning machine for both cases. The cutting conditions are given below. The workpiece surfaces are measured in *Mitutoyo Roundtest, RA-116*. The measurements are performed at specific location of workpiece (18,27,36 mm from

hub). The results of the comparison of the surfaces are tabulated in table 5.4 and roundness error versus location graph is in figure 5.5.

Cutting conditions
 Spindle speed : 900 rpm
 Feed : 0.15 mm/rev
 Feed overwrite : 50 %
 Depth of cut : 0.15 mm

Name of measurement	Measurement Location From Hub (mm)	No control (μm)	Constant position control (μm)	Improvement (%)
Roundness (up to 15 UPR)	18	4.09	1.26	69.2
Roundness (Full UPR)	18	13.62	8.39	38.4
FFT (Principal UPR)	18	1.76 (2 UPR)	0.55 (2 UPR)	68.8
Roundness (up to 15 UPR)	27	4.92	2.47	49.8
Roundness (Full UPR)	27	14.85	10.01	32.6
FFT (Principal UPR)	27	1.90 (2 UPR)	0.85 (2 UPR)	55.2
Roundness (up to 15 UPR)	36	4.35	2.46	43.4
Roundness (Full UPR)	36	13.47	9.44	29.9
FFT (Principal UPR)	36	1.89 (2 UPR)	0.94 (2 UPR)	50.3

Table 5.4 (Example 1): Comparison of measurement between PBCD control cutting and no control cutting

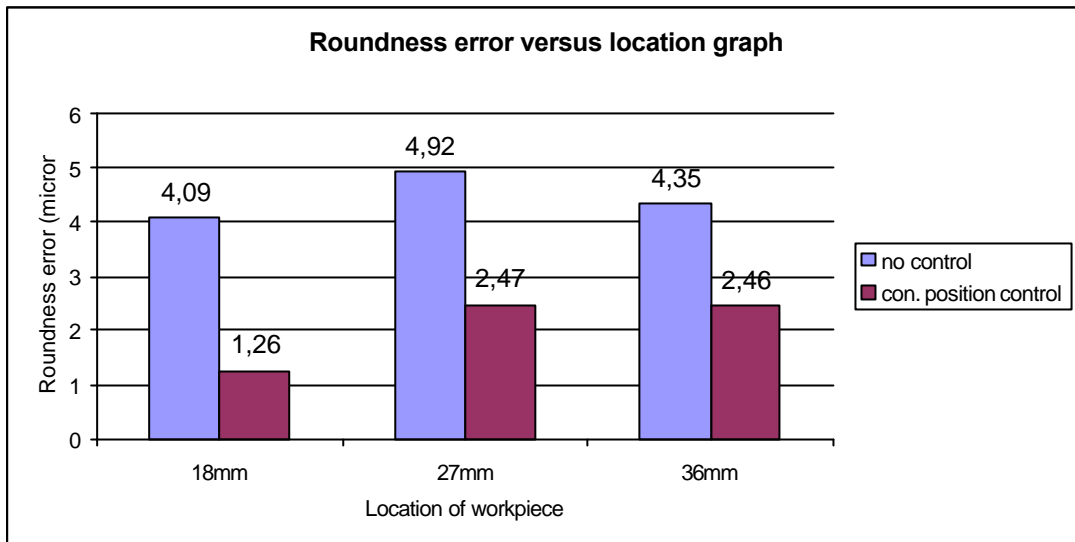


Figure 5.5 (Example1) Comparison of roundness error between PBCD control and no control

It can be concluded from the figure and table that the roundness error is decreased up to 30 % of the no control cutting case when constant position control is used in the cutting. Also the amplitudes of the principle UPR values (2 UPR) are decreased to 40 % of the no control cutting case.

Example 2

This example is nearly same with Example 1. Again the performance of the PBCD under constant position control with respect to no control is investigated. But the cutting conditions are different now. These are given below. The measurements are performed at specific location of workpiece (9,27,36 mm from hub). The results of the comparison of the surfaces are tabulated in table 5.5 and roundness error versus location graph is in figure 5.6.

Cutting conditions

Spindle speed	: 1464.844 rpm
Feed	: 0.2 mm/rev
Feed overwrite	: 30 %
Depth of cut	: 0.1 mm

Name of measurement	Measurement Location From Hub (mm)	No control (μm)	Constant position control (μm)	Improvement (%)
Roundness (up to 15 UPR)	9	1.74	1.13	35.1
Roundness (Full UPR)	9	10.63	11.47	-7.3*
FFT (Principal UPR)	9	0.43 (3 UPR)	0.28 (2 UPR)	34.9
Roundness (up to 15 UPR)	27	2.09	1.15	45.0
Roundness (Full UPR)	27	11.51	13.32	-13.8*
FFT (Principal UPR)	27	0.56 (2 UPR)	0.25 (2 UPR)	55.4
Roundness (up to 15 UPR)	36	1.66	1.27	23.4
Roundness (Full UPR)	36	11.26	10.93	2.9
FFT (Principal UPR)	36	0.42 (3 UPR)	0.42 (2 UPR)	0

Table 5.5 (Example 2): Comparison of measurement between PBCD control cutting and no control cutting

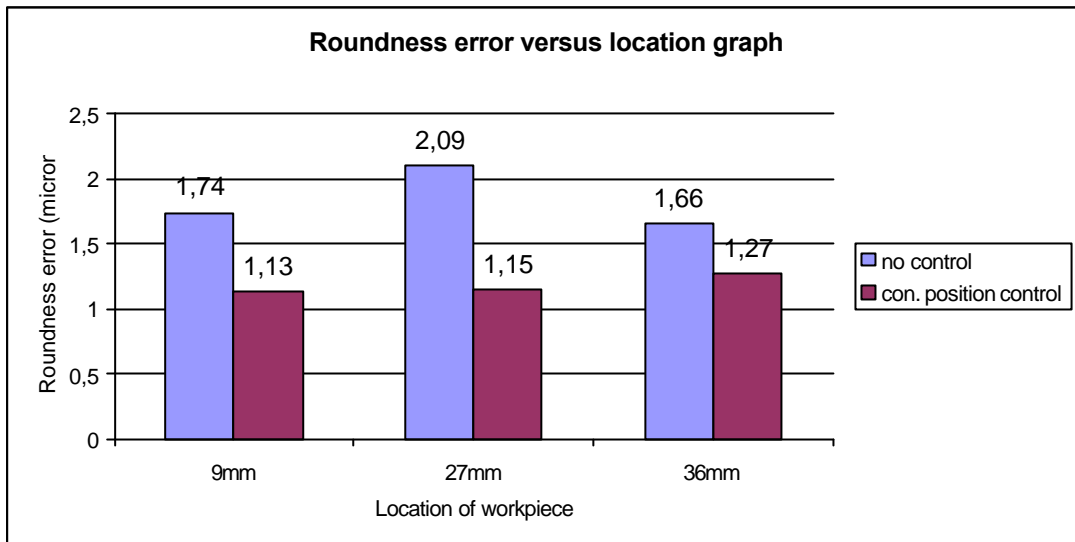


Figure 5.6 (Example2) Comparison of roundness error between PBCD control and no control

In this example, the improvement in the roundness error is now in the order of 25-45 %. This improvement difference from example 1 improvement can be explained from different cutting conditions of two cases. Also the values with asterisks show negative improvements. These negative values are due to the chattering effects of cutting conditions on the surface. But as explained in the previous sections, chattering does not contribute the form error. It effects only the surface roughness.

Example 3

In order to see the effect of filter on control, the measurements after cutting using constant position control with filtered feedback data, is compared with the one that is not filtered. In constant position control with filter case, Chebyshev I (with low pass cut-off frequency 1 rad/sec (0.16 Hz), and order of one) is used. The measurements are performed at specific location of workpiece (18,27,36 mm from hub). The other conditions are same with Example 2. Results are shown in table 5.6 and in figure 5.7.

Cutting conditions

Spindle speed : 1464.844 rpm
 Feed : 0.2 mm/rev

Feed overwrite : 30 %
 Depth of cut : 0.1 mm

Name of measurement	Measurement location from hub (mm)	Constant position control without filter (μm)	Constant position control with filter (μm)	Improvement (%)
Roundness (up to 15 UPR)	18	4.75	2.28	52.0
Roundness (Full UPR)	18	13.65	12.65	7.3
FFT (Principal UPR)	18	0.93 (3 UPR)	0.74 (2 UPR)	20.4
Roundness (up to 15 UPR)	27	4.82	1.64	66.0
Roundness (Full UPR)	27	16.06	11.81	26.46
FFT (Principal UPR)	27	1.05 (3 UPR)	0.5 (2 UPR)	52.4
Roundness (up to 15 UPR)	36	4.71	1.51	67.9
Roundness (Full UPR)	36	14.97	13.25	11.5
FFT (Principal UPR)	36	0.90 (3 UPR)	0.35 (2 UPR)	61.1

Table 5.6 (Example 3): Comparison of measurement between PBCD control cutting and no control cutting

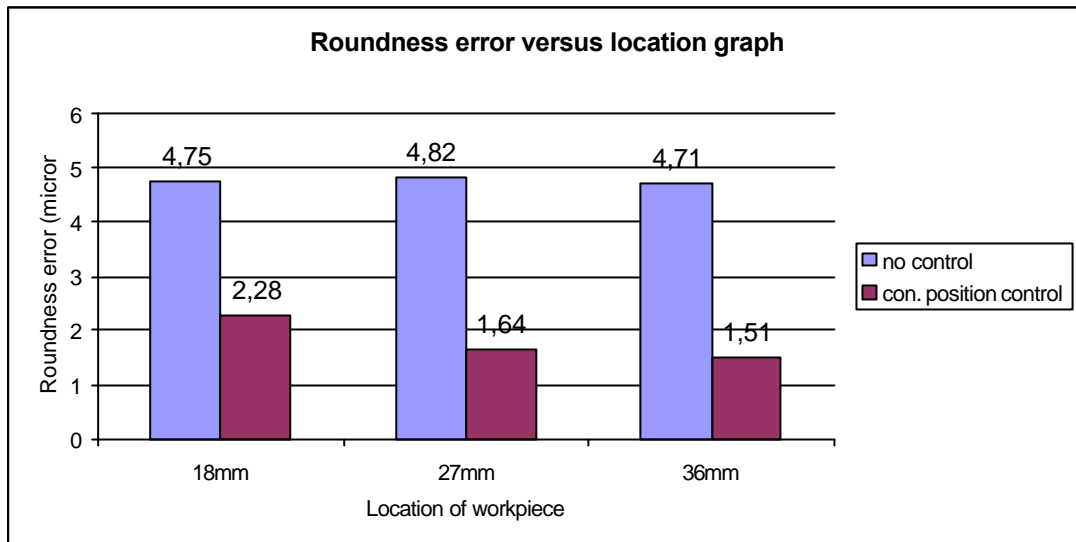


Figure 5.7 (Example3) Comparison of roundness error between PBCD control with filter and the one without filter

It can be concluded from the figure and table that the roundness error is decreased up to 68 % of the constant position control without filter cutting case when the one with filter is used in the cutting. Also the amplitudes of the principle UPR values (2 or 3 UPR) are decreased to 20 % of the constant position control without filter cutting case. These results show that the filter is effective on the surface of the workpiece.

Example 4

Comparison of constant position control of the PBCD with the no control of the one regarding the variation of diameter is investigated too. This example is performed to see how the diameter variation of the workpiece along the length is changing when constant position control is used in the cutting. The nominal diameter of both cases is chosen nearly same (37.5-38mm). In this example, the measurements are done using *Aeroel slit laser*. The cutting conditions are same with Example 2 and 3. The cutting conditions, table and corresponding figure are given below (Table 5.7), (Figure 5.8);

Cutting conditions

Spindle speed	: 1464.844 rpm
Feed	: 0.2 mm/rev
Feed overwrite	: 30 %
Depth of cut	: 0.1 mm

Location of measurement	Diameter (mm) no piezo control	Diameter (mm) piezo control	Variation (̂ m) no piezo control	Variation (̂ m) piezo control
5mm	37.4697	38.0210	0	0
10mm	37.4686	38.0183	-1.1	-2.7
15mm	37.4645	38.0171	-5.2	-3.9
20mm	37.4624	38.0170	-7.3	-3.9
25mm	37.4615	38.0165	-8.2	-4.5
30mm	37.4632	38.0193	-6.5	-1.7
35mm	37.4668	38.0195	-2.9	-1.5
40mm	37.4664	38.0183	-3.3	-2.7

Table 5.7 (Example 4): Comparison of diameter measurement between PBCD control cutting and no control cutting

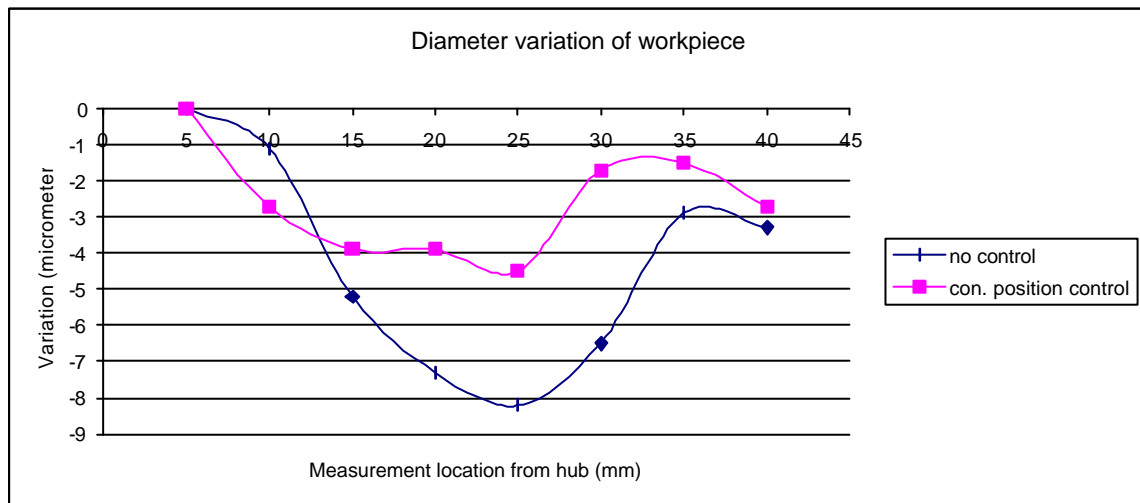


Figure 5.8 Diameter variation of workpiece between no control and constant position control case

This example shows the difference of the workpiece diameter variation of constant position control to no control of PBCD. The figure shows that the maximum diameter variation of constant position control is decreased to nearly half of the no control of PBCD. The other important result inferred from the figure is that the overall trends of both cases are nearly same.

5. 3. DYNAMIC POSITION CONTROL OF PBCD

Dynamic position control is the control algorithm written in dSPACE software. In this control, a sinusoidal input value, which has calculated frequency and amplitude according to the harmonics explained in previous sections of the workpiece roundness error, is given to the PBCD. The main purpose of this control is to keep the PBCD tool tip in sinusoidal motion that would be reverse of the harmonics of the roundness error on the workpiece during cutting. So that, by using this control the specified roundness harmonic is eliminated during in the cutting operation. But the nature of the operation is dynamic, it creates problems such as noise, chattering and control error.

In dynamic position control of PBCD, the surface characterisation changes, after cutting is investigated (Figure 5.9). The corresponding simulink program is given in the Appendix. In the program, the sine wave input command is dependent upon the encoder of the step motor of CNC machine spindle. Encoder position of step motor is measured by DS1102ENC_POS block. In order to get radian angle value this block is multiplied by radian gain which is $-(2^{21}).2.\pi/(1024)$. Where 1024 is the ppr (parts per revolution) of encoder. Since one location must be known exactly, index point of encoder is found by the block DS1102ENC_INDEX_C. If index is found, the block is set to 1. So if it is equal to 1, the encoder position starts from index point. Then the position can be converted to degrees by multiplying by degree gain $(360/(2*\pi))$.

There are lots problems in this operation. One of the main problems of dynamic cutting is the spindle motor of CNC machine. Because of the properties of the step motor, the speed comes to its command angular velocity approximately 0.6 second after starting to turn. In order to overcome this settling time effect, 18000 degree of angle (50 full turn) is paused after starting to turn. So that the spindle is settled down to work in synchronisation with PBCD. Sine wave is ready to start to run into the control algorithm. However, step motor velocity ripple is in the order of 200 rpm. Another problem is that, step motor is turning at some fixed angular velocities. For instance, it is rotating around 1464.844 rpm when 1300-1600 rpm angular velocity command is given from G-code of CNC machine. One possible solution for

this problem is running step motor at these fixed velocities. If 1500 rpm spindle motion is needed, 1464.844 rpm is used at the G-code program. Then the piezo is operating according to this angular velocity of the spindle.

The control algorithm is the same as the constant position control algorithm that is explained in the constant position control of PBCD section except some parameters. First, PID parameters are $K_p = 120$, $K_i = 2000$, $K_d = 0.005$. Second, the filter is still Chebyshev I filter but the cut-off frequency is now higher than 500 rad/sec. Actually cut-off frequency is dependent on the application. If higher harmonic roundness errors are to be eliminated, higher cut-off frequency value is needed. For example, for trilobe roundness error compensation at the 1500 (25 Hz) rpm spindle speed, $25 \times 3 = 75$ Hz (471.24 rad/sec) frequency of piezo motion is required. In order to eliminate higher frequency noise, also considering the piezo frequency, cut-off frequency in the order of 700 Hz for low pass filter is enough to this application. Because of the higher frequency application, the amplitude of the piezo must be low compared to constant position control of PBCD. The higher the frequency of PBCD control, the more difficult to control PBCD. So the position error is getting higher as the sine wave frequency increases. The sampling period of dynamic position control of PBCD is found 45

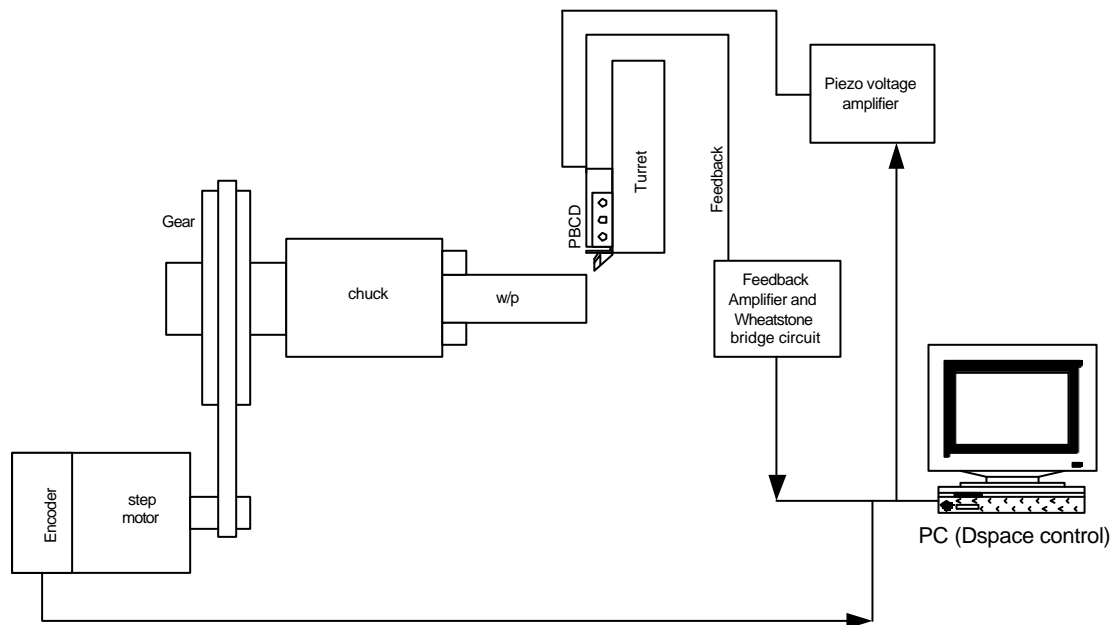


Figure 5.9 Dynamic position control of PBCD

Example 5

In this example, the performance of the PBCD under dynamic position control is investigated. Roundness errors and the lowest frequency form errors (2 UPR) of the surface at different locations along the length of workpiece are found. The cutting conditions and the amplitude of PBCD are given below. The workpiece surfaces are measured in *Mitutoyo Roundtest, RA-116*. The results of the comparison of the surfaces are tabulated in table 5.8 and roundness error versus location graph is in figure 5.10.

Cutting conditions

Spindle speed	: 1464.844 rpm
Feed	: 0.2 mm/rev
Feed overwrite	: 10 %
Depth of cut	: 0.1 mm
Amplitude of PBCD	: 2.5 μ m

Location (μ m)	Roundness (up to 15 Upr) (μ m)	FFT (2 upr) (μ m)
5	4.60	1.03
10	5.23	1.33
15	3.68	1.99
20	1.78	0.60
25	7.23	1.80
30	4.67	1.08
35	4.76	0.64
40	2.58	1.14
45	1.65	0.46
50	4.40	0.97

Table 5.8 (Example 5): Dynamic position control results of PBCD

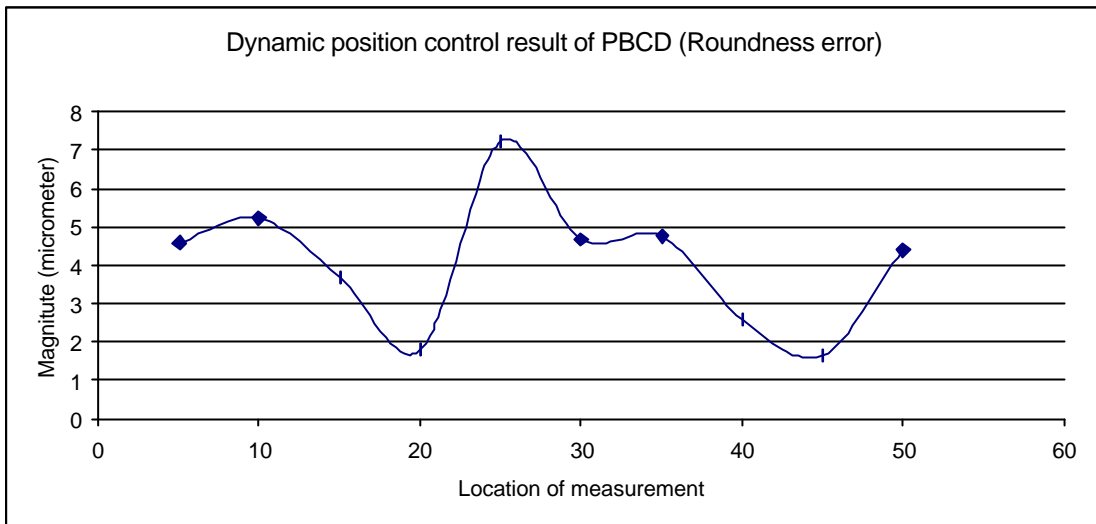


Figure 5.10 Dynamic position control results of PBCD

It can be concluded from the figure and table that the roundness error is highly deviating when dynamic position control is used in the cutting. The maximum roundness error is found as 7.23 along the length and the high roundness errors are due to the problems of dynamic position control of PBCD, which is explained above. Therefore the results are not so good.

CHAPTER 6

CONCLUSION AND FUTURE WORK

In this study, sources of errors in a turning system are analysed. A potential compensation system using precision cutting with piezo based cutting device (PBCD) in CNC turning machine is presented. In order to develop and demonstrate the system several experiments were done by utilising software and hardware tools such as Labview, simulink and dSPACE software, laser displacement sensor, thermocouple, slit laser, roundness measuring machine, piezoelectric actuator, amplifier circuit, dynamic signal analyser, Catia V.5., AutoCad 2000. PBCD is a PID (Proportional Integral Derivative) controlled both for constant position and dynamic position operation. Constant position control operation can be used for diameter errors. In constant position control, the cutting operation is proved to be satisfactory. Roundness of workpiece at different sections are improved at least 25-30 % with respect to non-control PBCD cutting. In dynamic cutting, the encoder of the CNC turning machine is taken in the control loop also. The improvement of surface error due to dynamic cutting is limited.

There are some limitations for this work. First, the spindle motor of CNC turning machine creates two main problems for dynamic cutting. These problems are late response of motor and high variation of angular speed. Using delay-time at the control algorithm solves the former one, but controller can not solve the latter one. Implementing this work on some other CNC machines, which have servo motor spindle, would give better angular speed stability (less variation). Second, the chattering of the tool is another problem that gives bad surface (waviness surface) characteristics to workpiece. The basic reason for chattering is the high flexibility of housing. A better housing for PBCD could be designed to improve rigidity. Third, the CNC machine, which PBCD is mounted on, is not a precise turning machine. If the PBCD is performed in diamond turning, very small depth of cut (in the order of one-micrometer level) turning may be possible. Also the chuck has higher set-up errors. For example eccentricity of chuck is between 40-60 μm . So, in order to control roundness of workpiece, minimum 100 μm depth of cut is needed not to cause eccentricity. One of the major problems faced in the experiments is the mechanical noise of the spindle motor of CNC turning machine. Turret and tailstock of the

machine transfers this mechanical noise. Since the PBCD is mounted on the turret, the feedback sensor of piezo stack actuator picks the noise. Therefore, the control loop becomes unstable. The software filter in dSPACE program could not eliminate this noise especially in Dynamic position control of PBCD. Other solution methods have been also tried. It was observed that, using electric tape band between turret and PBCD contact points eliminate the noise by 95 %, also the metal screws connecting turret tool holder with housing of PBCD also transfer the noise. Then plastic screws are used instead of metal screws to lessen the noise in the control loop.

In the future, the idea of roundness error compensation can be implemented in in-process measurement and control systems. In this research, in-process measurements can not be done by using only one laser. For diameter and roundness of workpiece, at least three sensors are needed at the same cross-section of the workpiece. Also the laser sensor, with higher accuracy and resolution is needed in order to achieve better precision.

The application of this system would be used in most conventional CNC turning machines in industry. Especially, the companies that produce their products in mass production. Because in these CNC turning machines in mass production, the cutting conditions such as cutting speed and feed, tool geometry and vibration are not changed. Therefore the workpiece geometric errors are usually repeatable. So if repeated errors are found, this system would be highly productive while using in the dynamic position control.

The constant position control case would be used to cut cylindrical workpieces in the correct diameter value. If the PBCD is fixed at the turret in order to get high rigidity after constant position control command is given, very low deflection of PBCD can be seen. So the correct diameter of workpiece would be achieved. In this application CNC turning parameters should be exactly known to get good results.

For the actuation part of this research, some other alternatives can be used instead of piezo stack actuators such as motors and linear motors. But these actuators have some disadvantages. For example, motor may be highly accurate but it needs a mechanical attachment for converting rotation to linear motion. These mechanical attachments would result in non-linearity (backlash, pitch resolution, friction) to the system. Also dc motors having low mechanical time constant for Dynamic position control can not be found easily. Likewise linear motor has some drawbacks. First, linear motors are not highly force resistive. They can be easily damaged from cutting

forces as the forces are directly applied on the motor. Second linear motors, have less bandwidth than piezo stack actuators and the bandwidth becomes limited when mechanical attachment or tool tip is inserted on linear motors. Lastly, they are not designed for hazardous environments (high temperature, chips, cutting fluids); Very good sealing would be necessary.

REFERENCE LIST

- [1] H. W. Mergler and S. Sahajdak, "In-process optical gauging for numerical machine tool control and automated process." *Proc 3rd NSF/RANN Grantee's Conf. On Production Research and Industrial Automation*, Cleveland, OH, p. 57 (1975)
- [2] H. W. Mergler and S. Sahajdak, "In-process optical gauging for numerical machine tool control." *Proc. 3rd Int. Conf. On Automated Inspection and Product Control*, University of Nottingham, April, p. 57 (1978).
- [3] T. Yandayan and M. Burdekin, "In-process dimensional measurement and control of workpiece accuracy." *International Journal of Machine Tools & Manufacture*, Vol. 37, No. 10 pp. 1423-1439, (1997).
- [4] Wen-Hong Zhu, Martin B. Jun, Yusuf Altintas, "A fast tool servo design for precision turning of shafts on conventional CNC lathes." *International Journal of Machine Tools & Manufacture*, Vol. 41, pp. 953-965, (2001).
- [5] C. James Li. and S. Y. Li, "To improve workpiece roundness in precision diamond turning by in situ measurement and repetitive control." *Mechatronics*, Vol. 6, No. 5, pp. 523-535, (1996).
- [6] Jeong-Du Kim, Dong-Sik Kim, "Waviness compensation of precision machining by piezo-electric micro cutting device." *International Journal of Machine Tools & Manufacture*, Vol. 38, pp. 1305-1322, (1998).
- [7] A. M. Shawky and M. A. Elbestawi, "In-process evaluation of workpiece geometrical tolerances in bar turning." *International Journal of Machine Tools & Manufacture*, Vol. 36, pp. 33-46, (1996).

[8] Eric H. K. Fung, S. M. Cheung, T. P. Leung, "The implementation of an error forecasting and compensation system for roundness improvement in taper turning." *Computers in Industry*, Vol. 35, pp.109-120, (1998).

[9] Xiaoli Li, R. Du, "Analysis and compensation of workpiece errors in turning." *Int. J. Prod. Res.*, Vol. 40, No. 7, pp. 1647-1667, (2002).

[10] Chih-Hao Lo, Jingxia Yuang, Jun Ni, "An application of real-time error compensation on a turning center." *International Journal of Machine Tools & Manufacture*, Vol. 35, No. 12, pp. 1669-1682, (1995).

[11] Keyence Catalogue, Sensors vision systems & measuring instruments' pp.321, (2000-2001).

[12] Mitutoyo User's Manual, RA-116 Roundness Measuring Machine, No. 99MBB002 A2.

[13] http://www.physicinstrumente.com/tutorial/4_21.htm

[14] Piezomechanik GmbH Catalogue, Piezoelectrical and Electrostrictive Stack Actuators and Ring Actuators.

[15] Richard S. Filiola, Donald E. Beasley, Theory and Design for Mechanical Measurements. John Wiley & Sons, New York, 2000.

[16] Katsuhiko Ogata, Modern Control Engineering, Fourth Edition, Prentice-Hall, New Jersey 2002.

[17] David J. Whitehouse, Handbook of Surface Metrology, IOP Publishing, Rank Taylor Hobson Ltd, 1994

[18] EMCO Innovative machine tools, Software Description EMCO WinNC GE Series Fanuc 21 TB, Ref. No. EN 1902, Edition A2000-3.

- [19] Yusuf Altintas, A. Woronko, "A piezo tool actuator for precision turning of *CIRP Annals Manufacturing Technology*, Vol. 51, pp. 303-306, (2002).
- [20] Byung-Kwon Min, George O'neal, Yoram Koren, Zbigniew Pasek, "A smart boring tool for process control." *Mechatronics*, Vol. 12, pp. 1097-1114, (2002).
- [21] V. Portman, B.Z. Sandler, "High-stiffness precision actuator for small displacements." *International Journal of Machine Tools &Manufacture*, Vol. 39, pp. 823-837, (1998).
- [22] D. Gao, Y.X. Yao, W.M. Chiu, F.W. Lam, "Accuracy enhancement of a small overhung boring bar servo system by real-time error compensation." *Journal of the International Societies for Precision Engineering and Nanotechnology*, Article in press, (2002).
- [23] Sang-soon Ku, Gary Larsen, Sabri Cetinkurt, "Fast tool servo control for ultra-precision machining at extremely low feed rates." *Mechatronics*, Vol. 8, pp. 381-393, (1998).
- [24] Ramutis Bansevicius, Vytautas Giniotis, "Mechatronic means for machine accuracy improvement." *Mechatronics*, Vol. 12, pp. 1133-1143, (2002).
- [25] James F. Cuttino, Arthur C. Miller, Dale E. Schinstock, "Performance optimization of a fast tool servo for single-point diamond turning machine." *IEEE/ASME Transactions on Mechatronics*, Vol. 4, No. 2 pp. 169-179, (1999).
- [26] Wei Gao, Robert J. Hocken, John A.Patten, John Lovingood, Don A.Lucca, "Construction and testing of a nanomachining instrument." *Precision Engineering, Journal of the International Societies for Precision Engineering and Nanotechnology*, Vol. 24, pp. 320-328, (2000).

[27] Yuichi Okazaki, Tokio Kitahara, “NC Micro Lathe to Machine Micro-Parts.” *ANON*.

[28] Erward M. Trend, Paul K. Wright, *Metal Cutting*, Fourth Edition, Butterwoth-Heinemann, New Delhi 2000.

[29] Yusuf Altintas, *Manufacturing Automation*, Cambridge University Press, New York 2000.

[30] John A. Schey, *Introduction to Manufacturing Processes*, Second Edition, McGraw-Hill, New York 1987.

[31] http://klabs.org/DEI/References/design_guidelines/design_series/1265msfc.pdf.

[32] <http://www.nanotechsys.com>

[33] Gavin Chapman, *Ultra-precision Machining Systems; an Enabling Technology for Perfect Surfaces*, Moore Nanotechnology Systems.

[34] <http://www.cmmoptic.com/diamond.html>.

[35] Jiri Tlustý, *Manufacturing Processes and Equipment*, Prentice-Hall, New Jersey 2000.

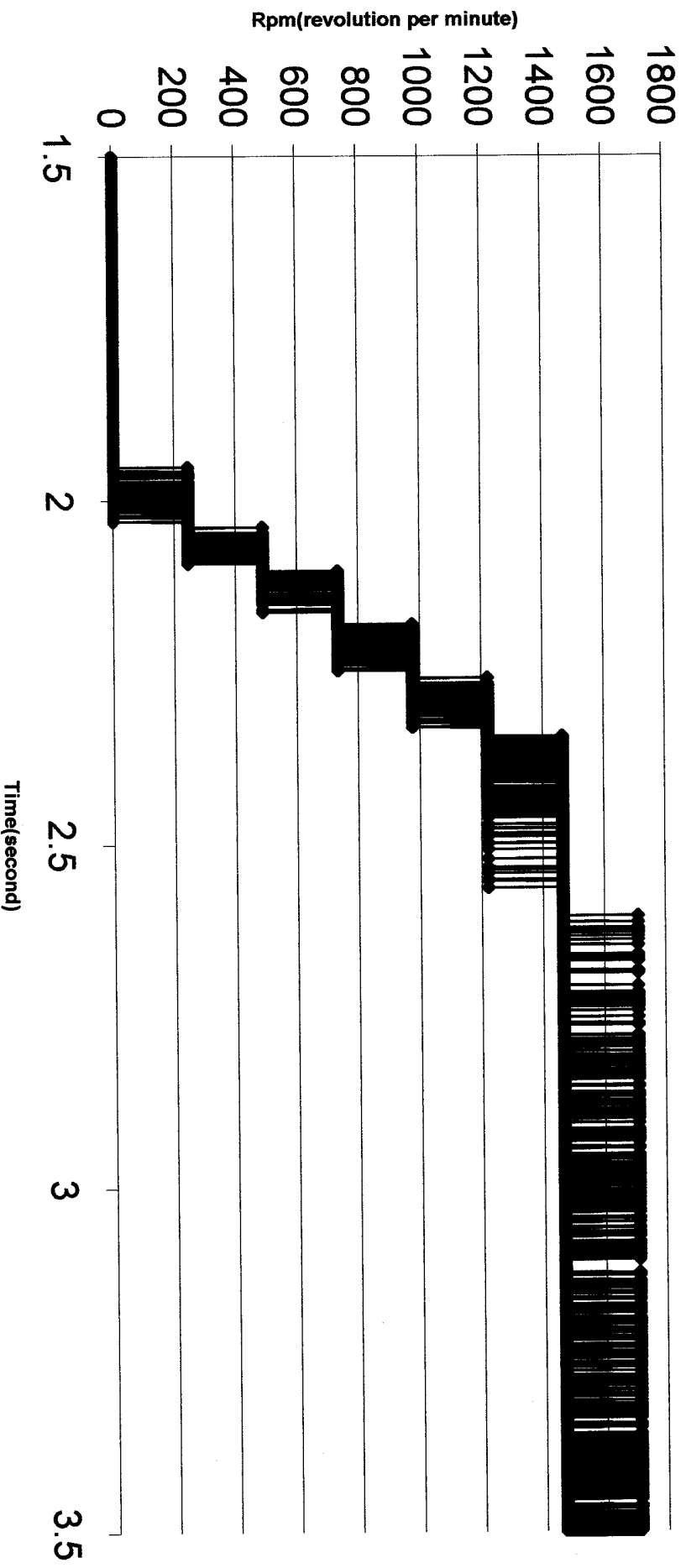
[36] Alexander H. Slocum, *Precision Machine Design*, Society of Manufacturing Engineers, Michigan 1992.

APPENDIX

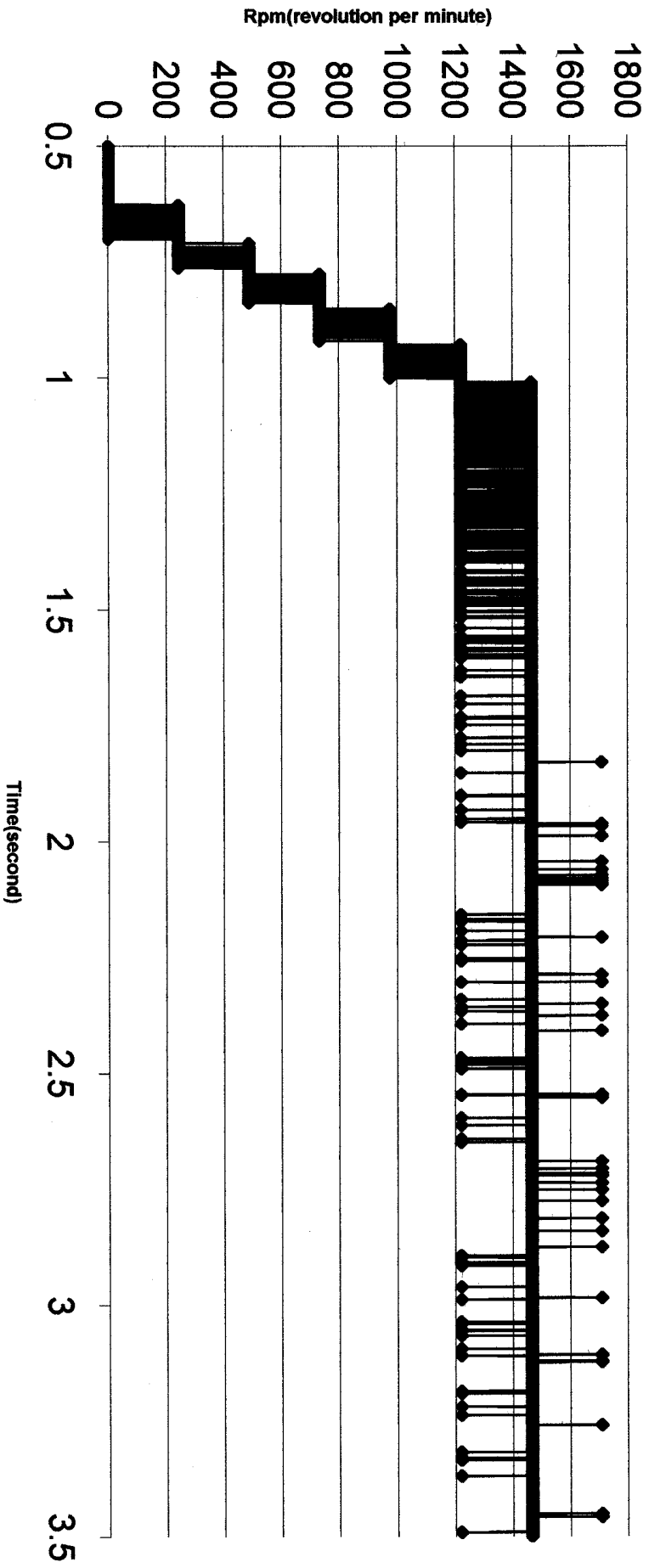
CNC G-code compensation program

O0066	'' Program name''
N5 G10 P0 Z-60.75	'' Data setting for workpiece zero point in z direction of CNC machine''
N10 G10 P0 W-61.4	'' Data setting for workpiece length''
N15 T0606	'' Turret tool number call''
N20 G97 S1500 F0.2 M4	'' Constant rotational speed 1500 rpm with 0.2 mm/rev and counterclockwise direction''
N25 G0 X48.9 Z-2	'' Positioning (rapid traverse) to X48.9 and Z -2, Compensation start''
N30 G1 X48.938 Z-50	'' Linear interpolation (feed) to X48.938 and Z 50, Compensation finish''
N35 G0 X60 Z50	'' Positioning (rapid traverse) to X60 and Z 50''
M30	'' Program end''

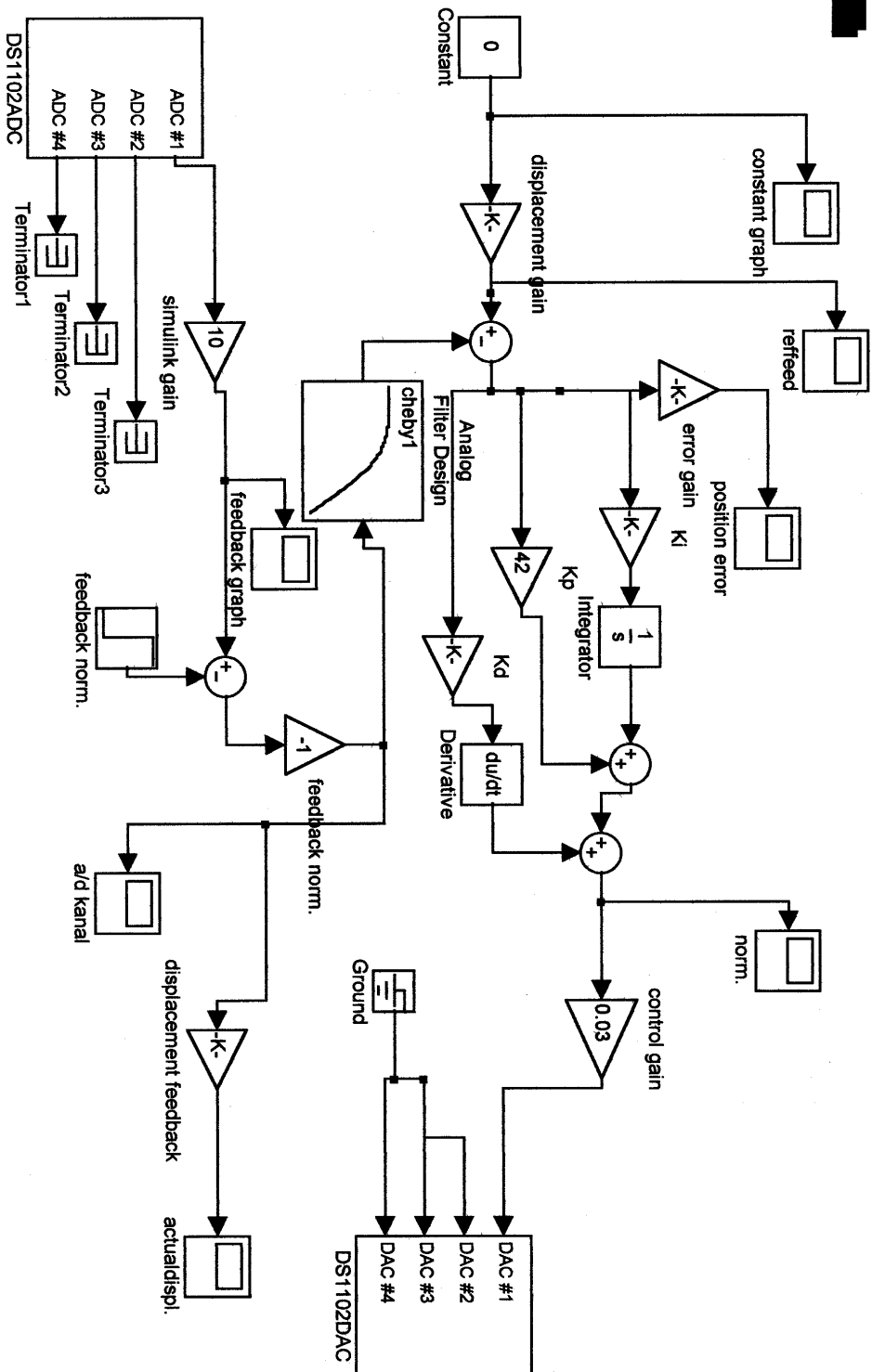
Angular velocity of CNC spindle motor (Command velocity 1500rpm)



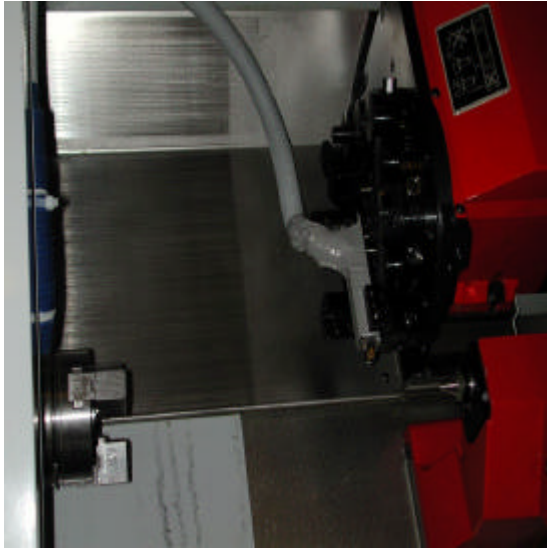
Angular velocity of CNC spindle motor (Command velocity 1464.844rpm)



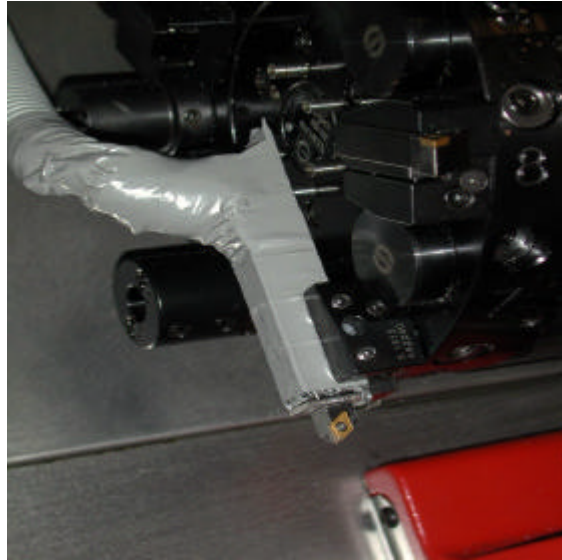
Static control of PBCD



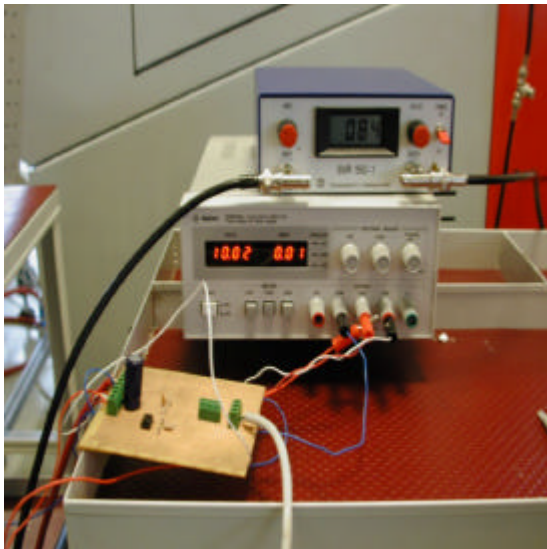
PICTURES OF PBCD AND ITS COMPONENTS



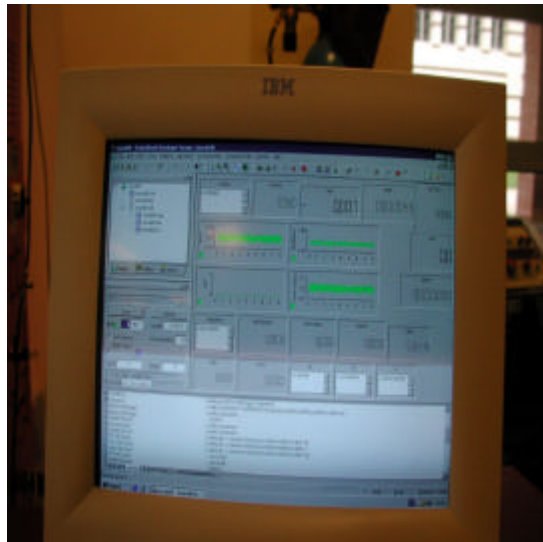
PBCD in CNC turning machine



PBCD on the turret of CNC machine



Piezo amplifier, power supply and feedback amplifier circuit



P.C. running dSPACE program